CHAPTER IV

RESULTS

In this study, GIS techniques of ArcView software are used to perform spatial databases for the spatial analyses of landslide assessment. The data sets related to landsliding in this study were derived from remote sensing data, available maps, and preliminary field investigation. As earlier in the previous chapters, the landslide susceptibility map, which is the result of landslide assessment analysis, was constructed using the factors related to landslide occurrence by bivariate probability and weighting methods. The method approach is based on the observed relationship between each landslide occurrence factor's class and past landslide events. The relationship between landslide (distribution) location and each landslide occurrence factor's class was analyzed in term of probability ratio of landslide occurrence. In addition, the weighted of importance of each factor was then determined based on probability ratio of landslide occurrence on each factor. The reliability of this method approach is directly dependent on the quality of factors data and landslide mapping.

In order to complete the factor analysis and to produce a landslide susceptibility map, three consecutive results are required. They are (1) Result of landslide information construction, (2) Result of landslide assessment analysis, and (3) Result of produce a landslide hazard zonation map.

4.1 Result of landslide Information Construction

All data are input into GIS as a spatial database of vector model (point) and raster format. These spatial databases, which are in part, the first output from this study, comprise the landslide location map and the factors map related to landslides.

4.1.1 Classification of Recent Landslides in Nan Province Area

Landslides occurring in the Nan Province study area on August 23, 2006 (see Figures 4.2 – 4.6), were triggered by continuous and heavy rainfall (with the total amount of 220 mm). This strong precipitation caused water from rainfall percolated through the weathered profile of bedrock and subsequently reduce its stability. These landslides are relatively shallow and mobilizing only the weathered profile of bedrock mixed with wood fragments, logs and water (Figure 4.1). Landslide sizes vary from small slumps of a few square-meter area to some of large landslides with surface areas in excess of one thousand square meters. This study considered that landslide occurrences are located close to the first-order stream and on the convex slope of mountain (Figure 4.2).

As a result, masses of weathered surface rocks, wood fragments, logs and muddy water moved quickly down from the mountain slopes to the low land areas. Some materials partly blocked the water, which flow from upper streams and then became saturated and liquefied by the water from the stream supplemented by the heavy rainfall, and were transformed into debris flow. Such debris flow moved quickly and violently downward along the channel or stream and pour out at the valley floor as a special muddy flood, which was a mixture of water, mud, sand, rock debris, and wood fragments (Figures 4.3-4.4). Landslide event at Nan Provincial area was classified as a complex shallow landslide with debris slide and flow using the classification of Cruden and Varnes (1996). Because the materials started to move as a debris slide, then combine with large amount of rainfall. A debris flow was taken place. This event damaged houses and properties, transportation lines and farmlands very seriously in several districts, such as Thung Chang, Chiang Klang, Na Noi and Na Mun district (Figures 4.5-4.6), As a result 6 peoples were killed and over 100 houses were completely destroyed.

In term of geological factor, the highest frequency of landslides occurring in the study area consists of sandstone intercalated with siltstone and

mudstone. Fractures in these rock mass and bedding planes of these sedimentary horizons act as weak zones which allow high amount and rate of infiltration of rain water. These weak zones cause the rocks to be subjected to high weathering and slope failures. Dips of bedding plane of the study area varying from 30° to 50° toward to the valley floor accelerated the slope failures. Field evidence suggested that vegetation covers did not have much resistance for sliding process in this area because the area was affected by sliding is mostly covered by moderate to dense vegetation. Extensive and perhaps illegal human activities in the form of agricultural activities and road excavations have also influenced the slope instability phenomena (Figure 4.7).

Figure 4.1 Shallow landslide of weathered surface at Nam Phoe Village, Thung Chang District, Nan Province.

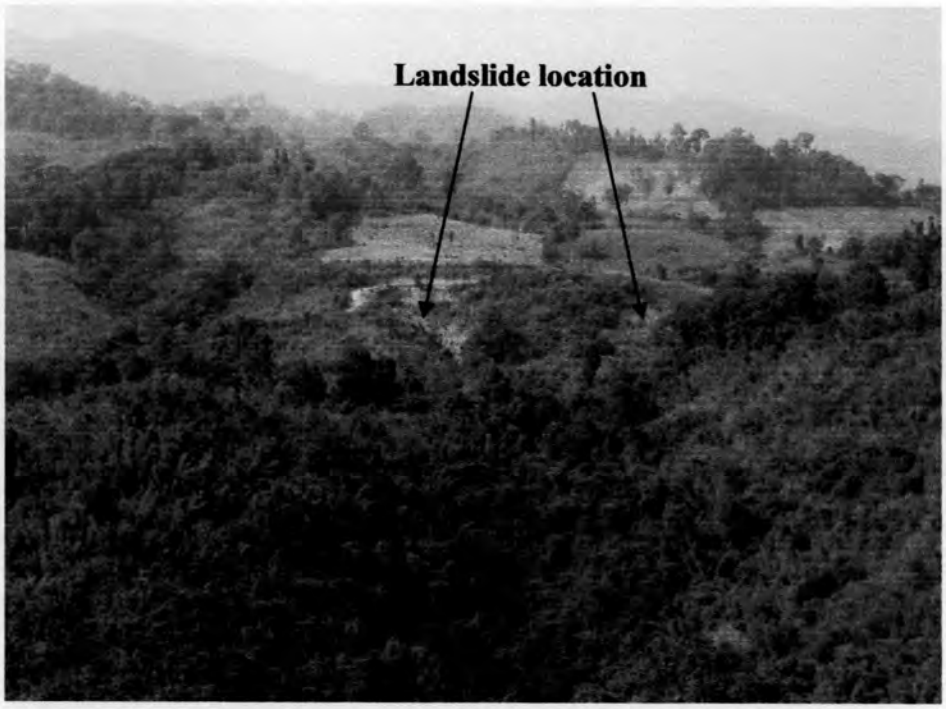

Figure 4.2 Initiation zone of two landslide scar occurring close to the mountainous ridge and the first order stream at Nam Phoe Village, Thung Chang District, Nan Province.

Figure 4.3 Large mixed masses of weathered surface rocks and wood fragments moved down from mountain slopes and stream valley to the low land area at Sop Pun Village, Chalerm Phrakiat District, Nan Province.

Figure 4.4 Debris flow moved downward along the channel and pour out at the valley floor at Ban Nam Phi, Thung Chang District, Nan Province, as a special muddy flood.

Figure 4.5 Nature of debris flow showing mixtures of poorly-sorted geological and non-geological materials at Sob Pun Village, Chalerm Phrakiat District, Nan Province.

Figure 4.6 Landslide damaging the road, electricity poles, and house at Nam Phi Village, Thung Chang District, Nan Province.

Figure 4.7 Human activities in the forms of deforestation and illegal agricultural proposes which influenced landslide. Note that this corn field is located at Huai Yen Village, Na Mun District, Nan Province.

4.1.2 Factors Map Related to Landslide and Database Construction

The output from this task is a result map of the existing landslide inventory and factor maps related to landslide occurrences. Various parameters affecting directly or indirectly to slope failure processes need to be analyzed and assessed. For landslide hazard zonation analysis, these include (1) geological factors, (2) topographical factors, (3) vegetation and land use / land cover factors, (4) hydrological factors and (5) landslide location map. Therefore, it is necessary to develop a digital spatial database, which comprises all variables affecting the occurrence of landslides, in the GIS format. All factors or maps are input to the GIS using ArcView GIS software as a spatial database.

In this thesis, the landslide distribution map is inputted and processed as a vector model (point) in GIS. The factor maps related to landslides, including lithological, lineament, elevation, slope angle, slope aspect, flow direction, land use / land cover, and NDVI unit maps are inputted and processed in GIS as a raster format with 30 x 30 meter grid. The study area comprises 13,528,880 grid cell numbers and 1,811 points of landslide locations. The spatial database of each factor is described below.

Landslide distribution map: Direct landslide mapping has been worked out using the Landsat 7 ETM and IKONOS satellite images. These data are acquired after the past landslide event and during the season of green vegetation. These types of imagery provide information of the ground surface, which is associated with landslide occurrence, such as landslide location and land use / land cover. Features including scarps, disrupted vegetation cover and deviation in soil moisture are generally conspicuous on the satellite image. These features are considered as landslide scars in this research work.

Landslide distributions were classified from the band combination of Landsat 7 ETM imagery for a small-size landslide. It is discovered from this study that

false-colored composites (FCC) based on combinations of the Landsat 7 ETM, bands 4 (near infrared - NIR), 5 and 7 (both shortwave infrared - SWIR) are suitable for clarifying features, were created by mass movements and can separate a bare soil from vegetated conditions and water (Figure 4.8). It is also found for the Nan study area that a 3 x 3-edge enhancement filter kernel was applied successfully to increase the contrast. Bare soil in this filtering image varies from light to dark blue depending on light incidence and moisture content, and the areas of forest (deep red) and cultivation (bright pink/orange) can be separated. A small difference in color is noted between landslides and other areas of bare soil (see Figure 4.8b). However, morphological evidences of a clear vegetated back scarp, a run out track and an accumulation zone was used to support the classification. Bare soils associated to morphology of the mass movements are assumed as landslide scars. So to summarized, the best results are achieved where the RGB 457 FCC data were examined by using a visual interpretation with the help of GIS technique.

As shown in Figure 4.8b; In the Nan area, there are two types of landslide scars determined based on sizes. One is the scars which are less than 50 meters in diameter and the other belongs to those with the surface areas more than 50 meters. It is quite clear from the result of the scar map that both types of landslide frequently occur in mountainous areas of the Pua basin. Particular area those in the vicinities of Chalerm Phrakiat, Thung Chang, Chiang Klang, and Pua districts.

Landsat 7 ETM image has fair spectral resolution, its 30 x 30 meters spatial resolution is low and generally not suitable for detailed landslide mapping. So using of IKONOS images have been used for visual interpretation to improve landslides detection from visual interpretation of Landsat 7 ETM image (Figure 4.9b). Because the landsat 7 ETM image has fair spectral resolution with the low spatial resolution of 30 x 30 meters so it is not suitable for detailed landslides mapping in this study. So IKONOS image was selected from MapPointAsia Website for visual interpretation to improve landslides detection from that of Landsat 7 ETM image

(Figures 4.9) because it creates the relatively high spatial resolution of 1 x 1 meter. This is suitable for small landslide scars mapping and morphology analysis related to landslides, such as run out track and accumulated zones. Once landslide locations from Landsat interpretation are verified and interpreted together with IKONOS image, it is found that some landslides are considered as relict features that have been inactive for many years. Good examples are at Nam Phoe village, Thung Chang district as shown in Figure 4.9b. They occupy areas of different vegetation types and densities from surrounding areas. But the most important part of providing data for the landslides distribution maps is a ground truth investigation, if the area is accessible. In this stage, some of marked landslide locations on the satellite images were checked with field observations. The marked locations that probably were not landslide scars, were removed. For the Nan study area, a total number of 1,676 landslide locations were identified from Landsat and IKONOS images (see Figure 4.8a and 4.9a). The additional ground truth checking detected 135 landslide locations (Figure 4.10a - 4.10d), which were not able to observe on satellite images such as landslides on the shadowed slopes and very recent landslides.

Finally, it is concluded based on the results of remote sensing interpretation and field survey that the landslide distribution map with 1,811 landslide locations was produced and input to GIS as a point format using Arc View software (Figure 4.11).

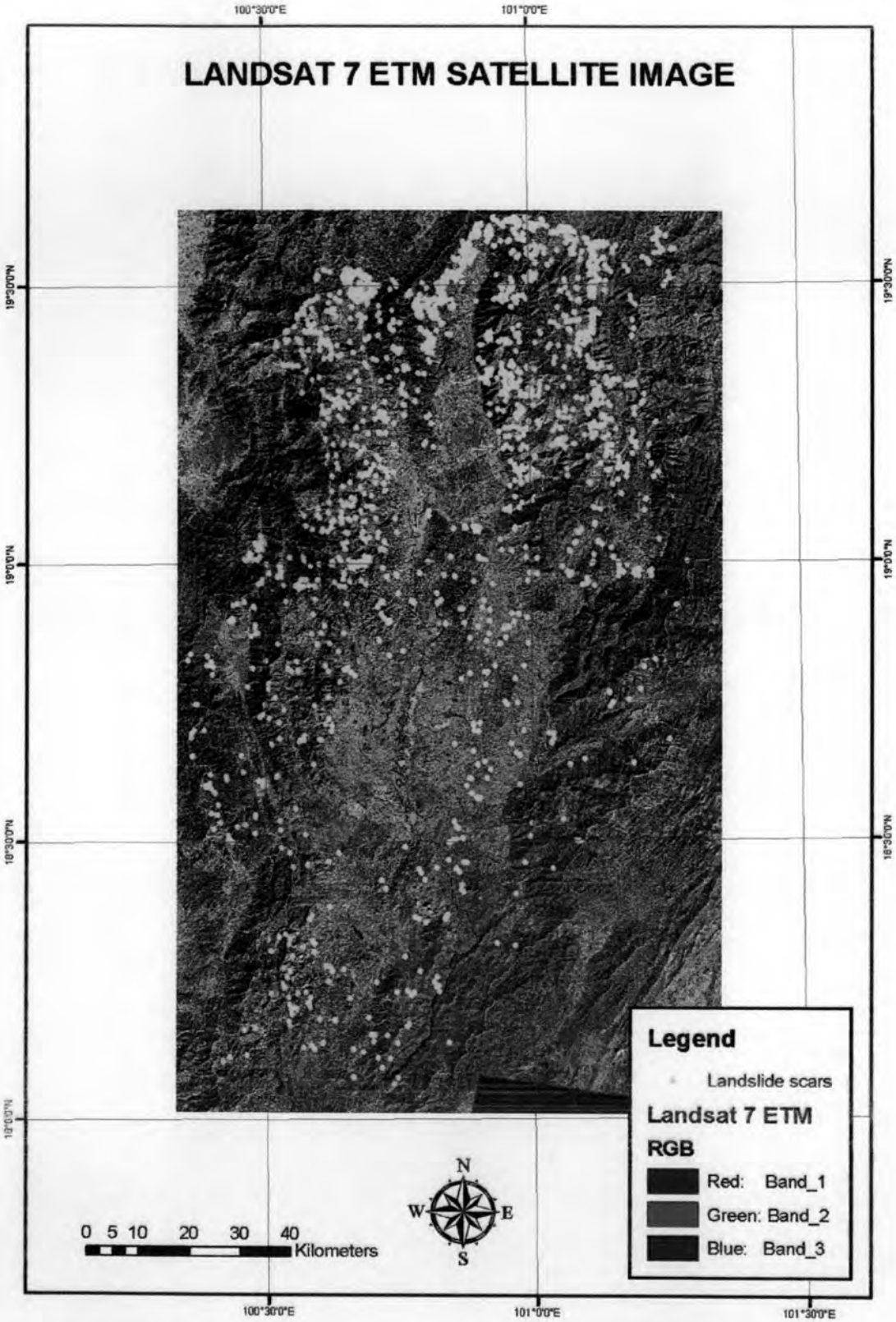

Figure 4.8a False-colored combinations of Landsat 7 ETM, B4, B5 and B7 image showing landslide scar location (yellow point) of the Nan study area. Note that Landsat 7 ETM images taken during Year 1999-2000.

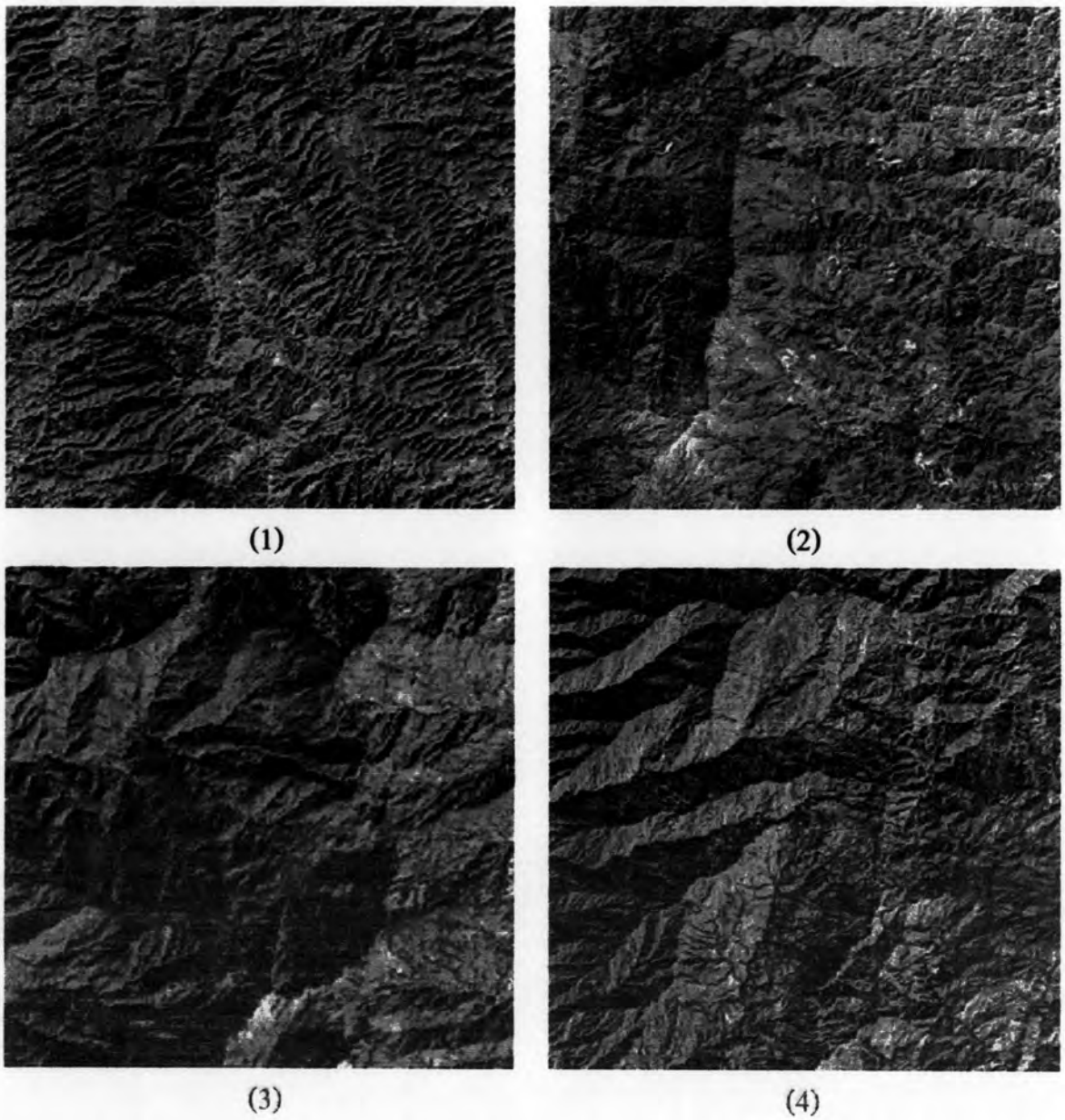

(1) (2)

(3) (4)

Figure 4.8b False-colored combinations of Landsat 7 ETM, B4, B5 and B7 image showing landslide scars those seen in vitual interpretation process; (1) landslide scars, (2) landslide scars, (3) large landslide scars, and (4) cultivation areas.

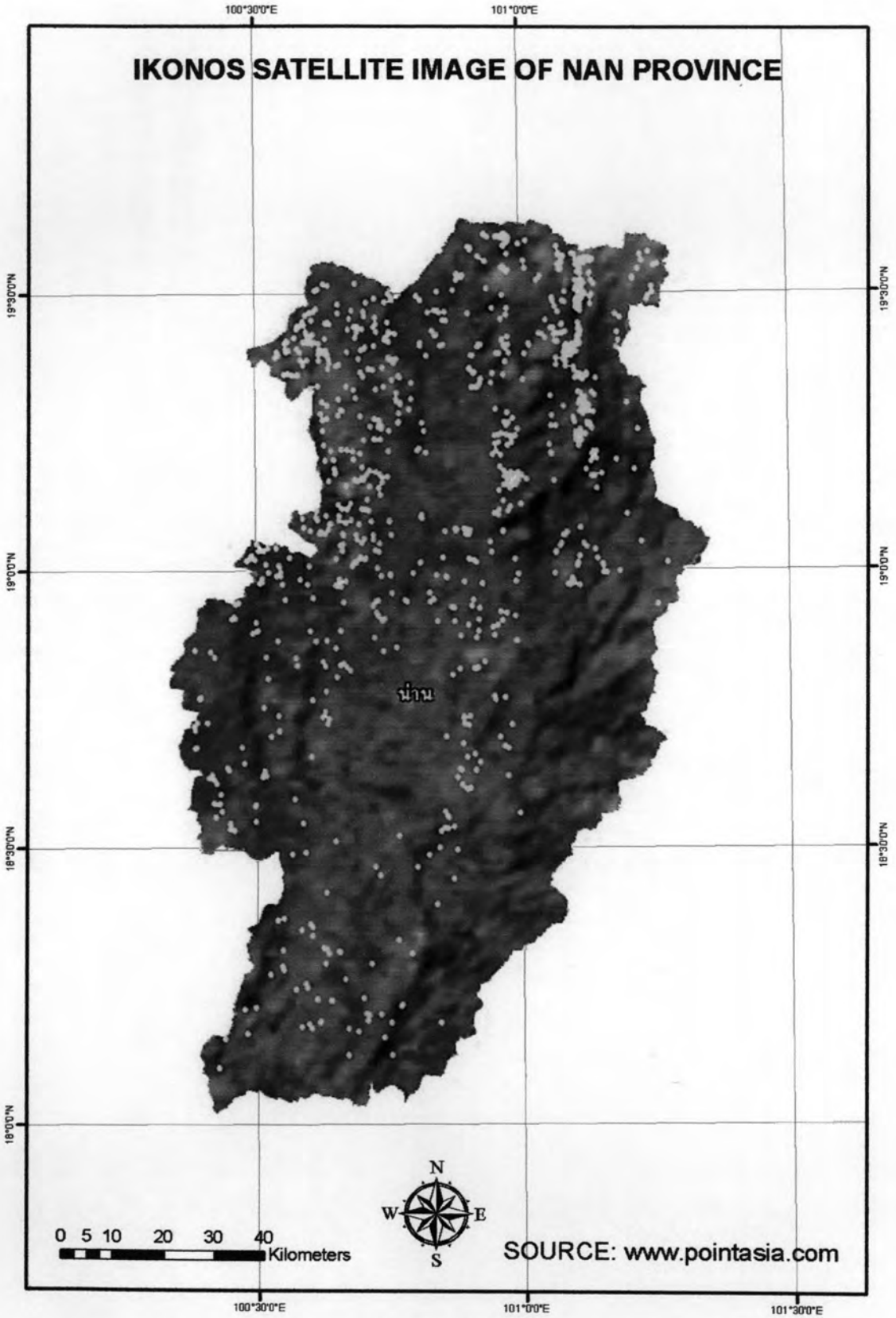

Figure 4.9a Landslide scar map of the Nan study area (yellow point) using IKONOS imagery interpretation. Note that IKONOS taken during Year 2003-2004.

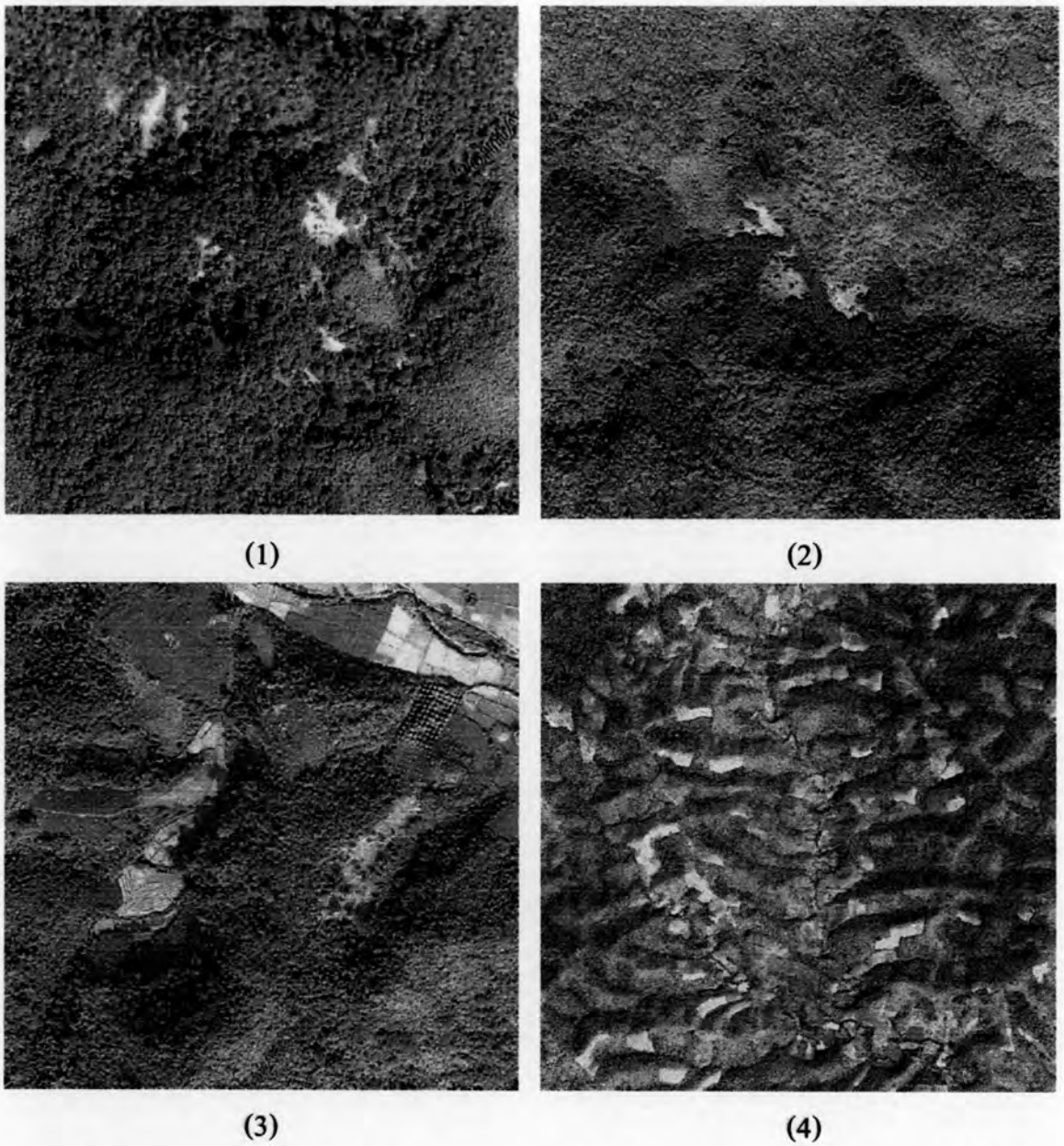

(1) (2)

(3) (4)

Figure 4.9b Landslide scar map of the study area (yellow point) using IKONOS imagery interpretation; (1) landslide scars, (2) large landslide scars, (3) large landslide scar and cultivation areas, and (4) cultivation areas.

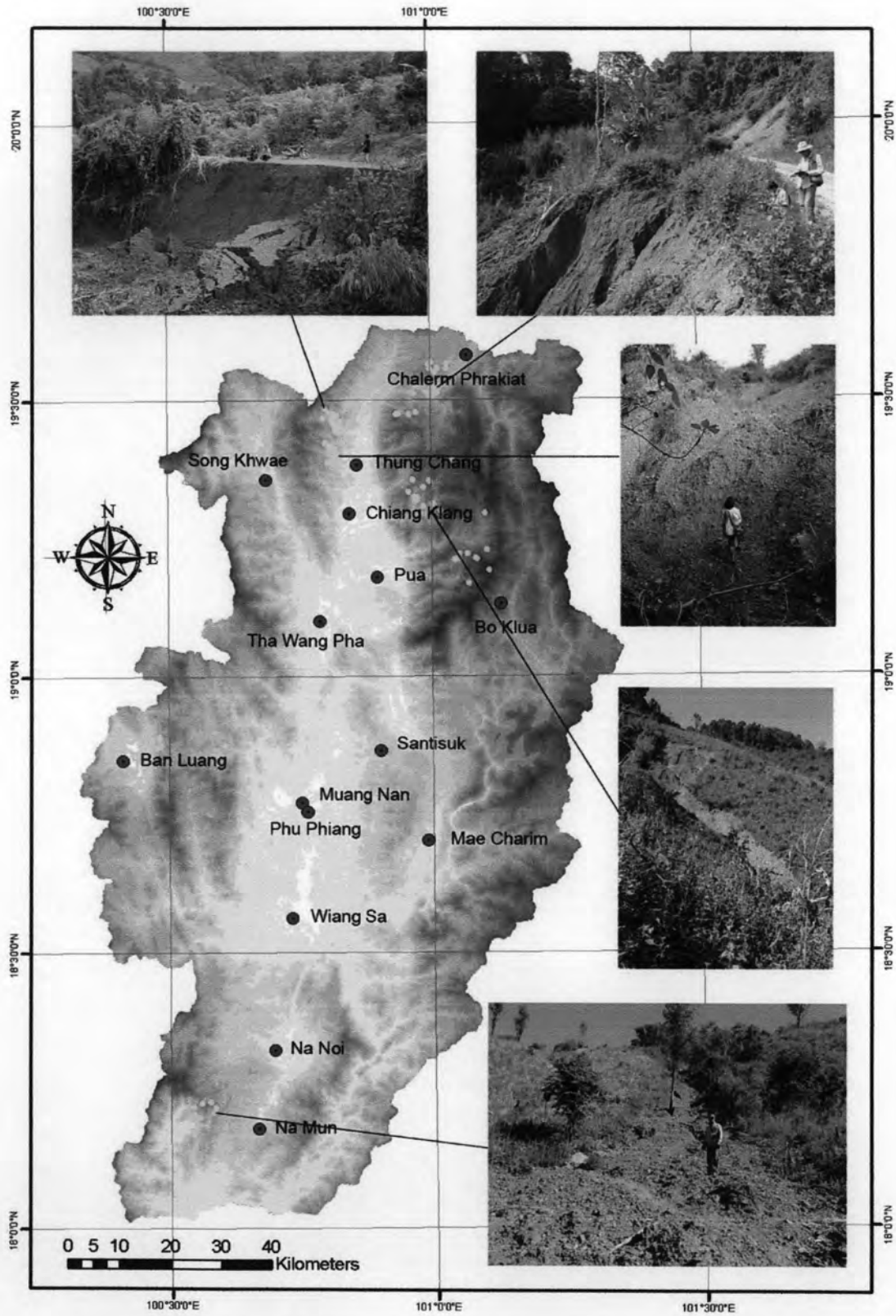

Figure 4.10a Landslide scar map of the Nan study area showing (yellow point) as observed in the field. Note that the photograph illustrating the recent landslides occurring during August, 2006.

Figure 4.10b Debris fall - landslide scars from field investigation in the Nan study area. (1) Pang Morn Village, Wiang Sa District (2) Ban Kok Village, Chiang Klang District (3) Nam Phoe Village, Thung Chang District.

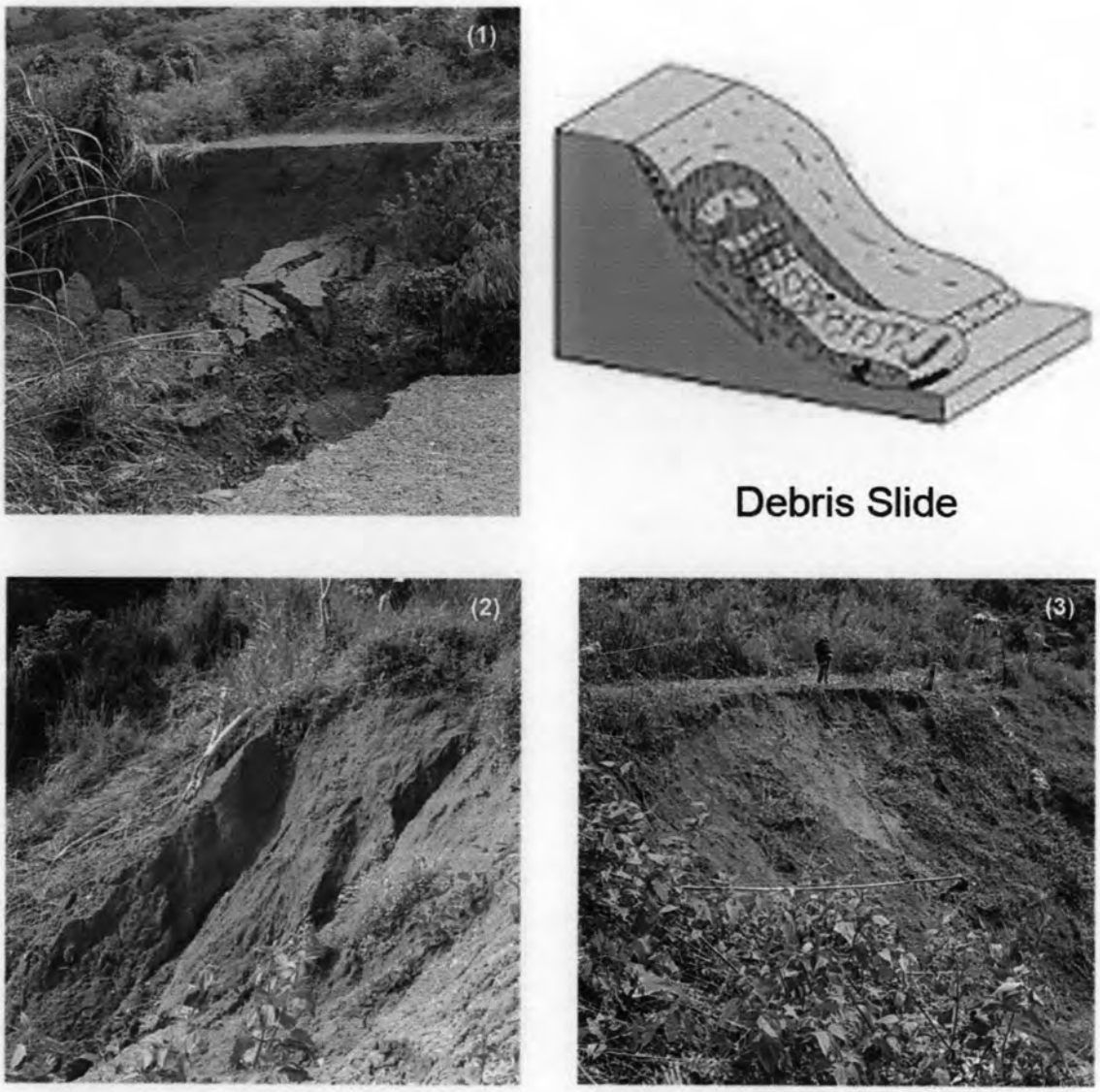

Figure 4.10c Debris slide - landslide scars from field investigation in the Nan study area. (1) Nam Phoe Village, Thung Chang District (2) Sop Pun Village, Chalerm Phrakiat District (3) Nam Phi Village, Thung Chang District.

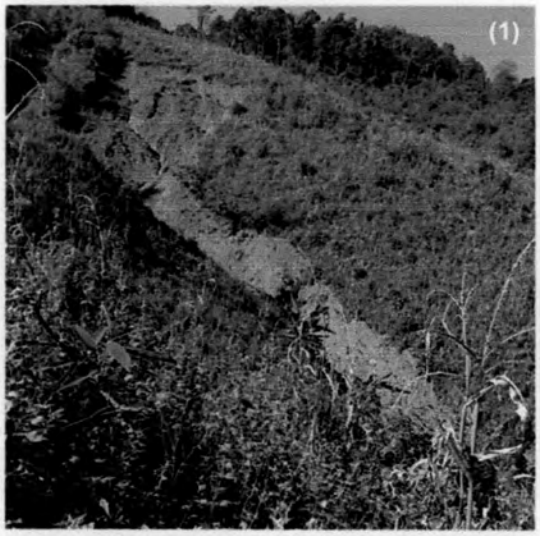

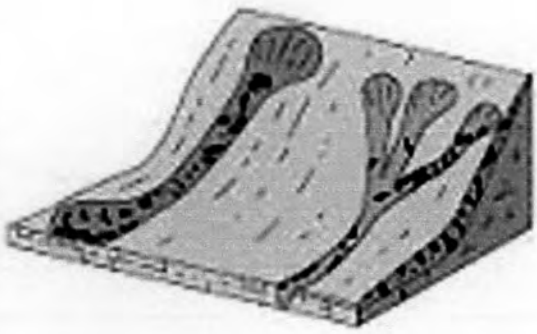

Debris Flow

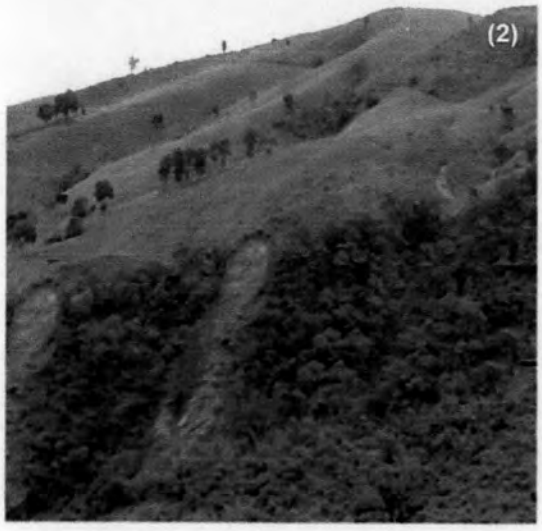

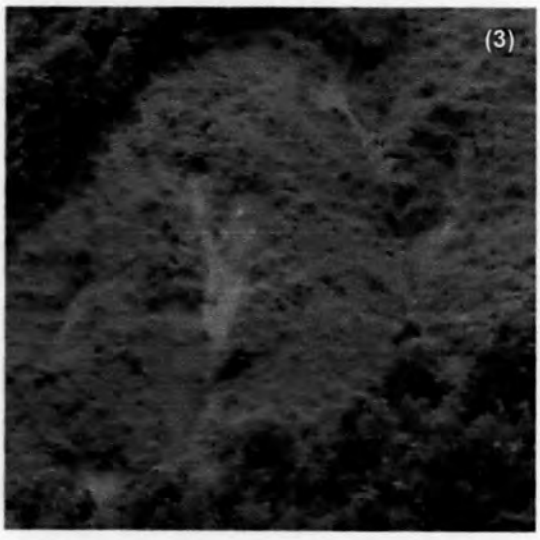

Figure 4.10d Debris flow - landslide scars from field investigation in the Nan study area. (1) Nam Phoe Village, Thung Chang District (2) Dong Pha Pun Village, Bo Klua District (3) Dong Pha Pun Village, Bo Klua District.

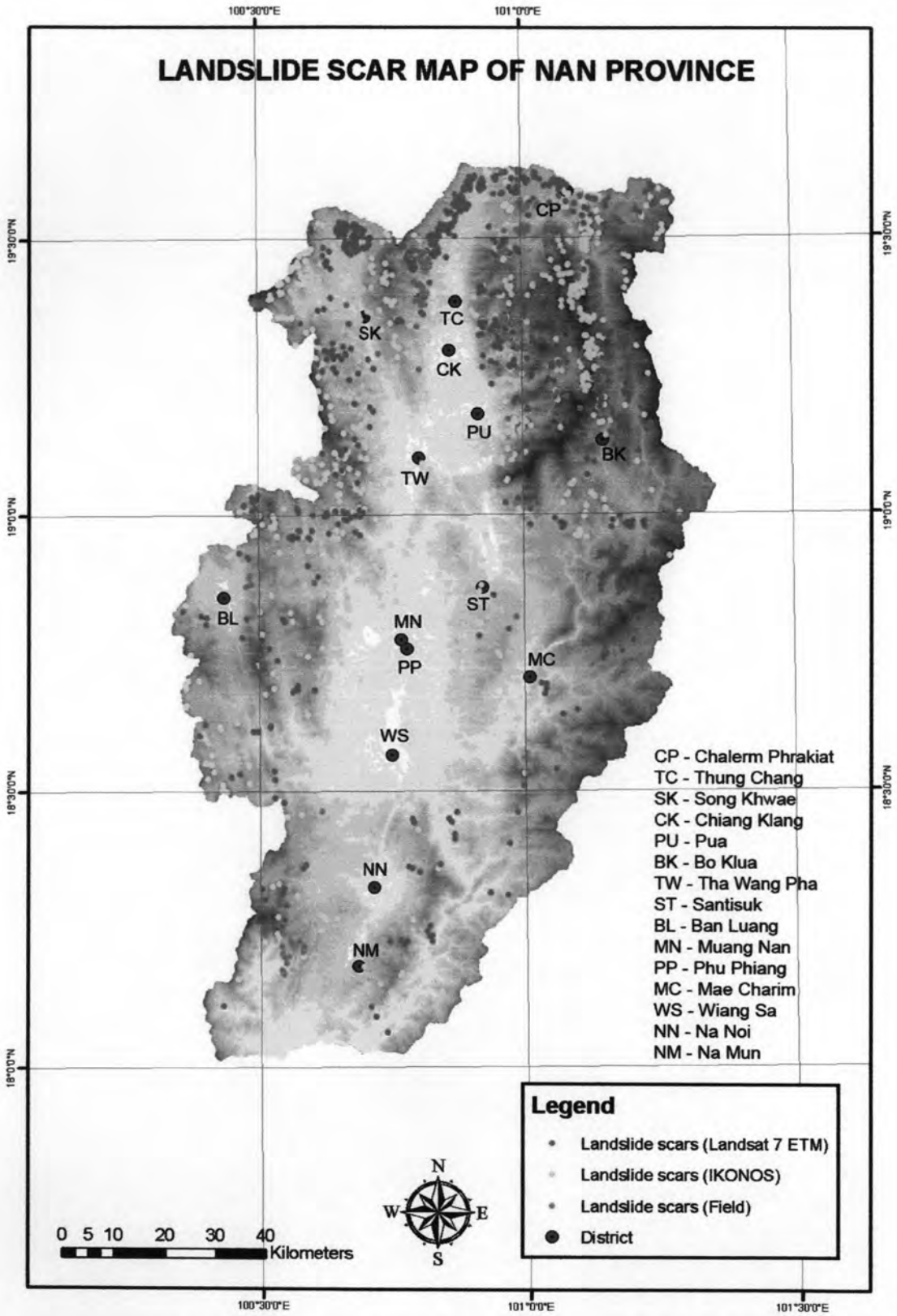

Figure 4.11 Landslide scar map of the Nan area of study showing locations of the past landslides 1,811 sites (blue, yellow, pink point), based on field data and remote sensing analyses.

Lithological map: In this study, geological boundaries are digitized from the published 1:50,000 scale geological maps contributed by the Department of Mineral Resources (DMR), Bangkok, Thailand. These geological maps are very good quality and fairly systematic and contain the geologically useful information. In general, rock units show a series of sedimentary, igneous, and metamorphic rock types. Various rock units ranging from the lower and upper Paleozoic, Mesozoic sedimentary and volcanic rocks to the younger unconsolidated sediments were noted in the study area (DMR, 1999). The previous geological maps of the study area preliminary compiled from the available reports, publications, and analogue maps, were used as a basic map. Traditionally, geological maps form a standard component in landslide hazard assessment analysis. However, stratigraphic legends of directly exist geological maps by themselves cannot be applied to these hazard assessment (Carrara et al., 1999). Conversion of these legends into an engineering classification is required (Van westen et al., 2008). Such classification can give more information on rock composition and rock mass strength (Carrara et al., 1999). Subdivision of formations often poses a problem, as intercalation of rock types cannot be properly mapped at medium scale (i.e. 1:50,000 scale). Therefore it is important to characterize rock types based upon field and laboratory analyses. So all the available geological maps were recompiled and transformed into lithological map. The compiled analogue maps were transformed into digital, via digitizing and edit by using ArcView-GIS software. Figure 4.13 show lithological map of the Nan study area.

In the present study, the classification of lithological units was based primarily on the hardness properties of rocks. The compressive strength value of each rock type (Hobbs, 1964; Attewell and Farmer, 1976; Roh and Reinhorn, 2008) and engineering properties of geological material (Guenther, 2003) are used to classify lithological units. In the present study, only some rocks were preliminary investigated for engineering properties. Unconfined fracture strength was tested for Nan rocks by using ASTM standard tests. These involve loading a small rock core until it fails

brittlely. The fracture strength is given as the maximum stress necessary to induce failure of the rock core called "Unconfined Compressive Strength (UCS)" value. This value gives an indication of the cohesiveness and density of a rock. Igneous, metamorphic and sedimentary rocks can be classified from very weak to very strong with regards to their unconfined fracture strengths. Generally, very weak to weak rock ranges from 0 - 40 MPa, medium rock ranges from 40 – 80 MPa, and strong to very strong rocks range from 80-320 MPa. The highest unconfined compressive strength observed in a rock is on the order of 400 MPa (e.g. nephritic jade) (Attewell and Farmer 1976). Moreover, some soil samples those collected from landslide locations in Nan Province have been tested in laboratory for UCS test. The UCS values of soil sample are used to combine with standard UCS value. From the preliminary UCS analysis, only 4 samples of sandstone and 1 sample of mudstone in the Nan study area were tested. The result conforms well with the range of the standard value of UCS unit shown in Figure 4.12. Then, lithological map of Nan Province area can be classified into 10 units (Table 4.1 and Figure 4.12) and was entered to GIS as a raster format using ArcView software (Figure 4.15).

As shown in Table A1 in Appendix A, coarse-clastic sediments seem to cover the Nan study area more than 4.8 million pixels or about 36% of the total area of lithology. The second rank of the lithological units is tuffaceous and volcanic rocks unit which occupy almost 3.6 million pixels or about 26.5% of the total area.

Table 4.1 Engineering properties of geological material for lithologic classification (Modified from Guenther, 2003).

Units	Lithologic unit	Friction[°]	Conductivity [m/hr]	Density[gr/cm^3]
1	Alluvial sediments	35 - 45	3.6 - 360	2 – 2.2
2	Terrace sediments	35 - 45	3.6 - 360	2 – 2.2
3	Semi-consolidated rocks	30 - 35	0.36 – 3.6	1.6 – 2
4	Very coarse-clastic rocks	35 - 40	0.36 – 3.6	1.6 – 2
5	Coarse-clastic rocks	30 - 35	0.36 – 3.6	1.6 – 2
6	Fine-clastic rocks	25 - 30	0.072 – 3.6	1.6 – 2
7	Limestone-dominated rocks	30 - 35	0.36 – 3.6	1.3 – 1.8
8	Granitic rocks	30 -35	0.36 – 3.6	1.6 – 2
9	Tuffaceous and volcanic rocks	25 - 30	0.072 – 3.6	1.6 – 2
10	Metamorphic and ultramafic rocks	35 - 40	0.36 – 3.6	1.6 – 2
Global Conductivity: 2.3 m/hr		**Global Friction:**33°	**Global Density:** 1.7 g/cm3	

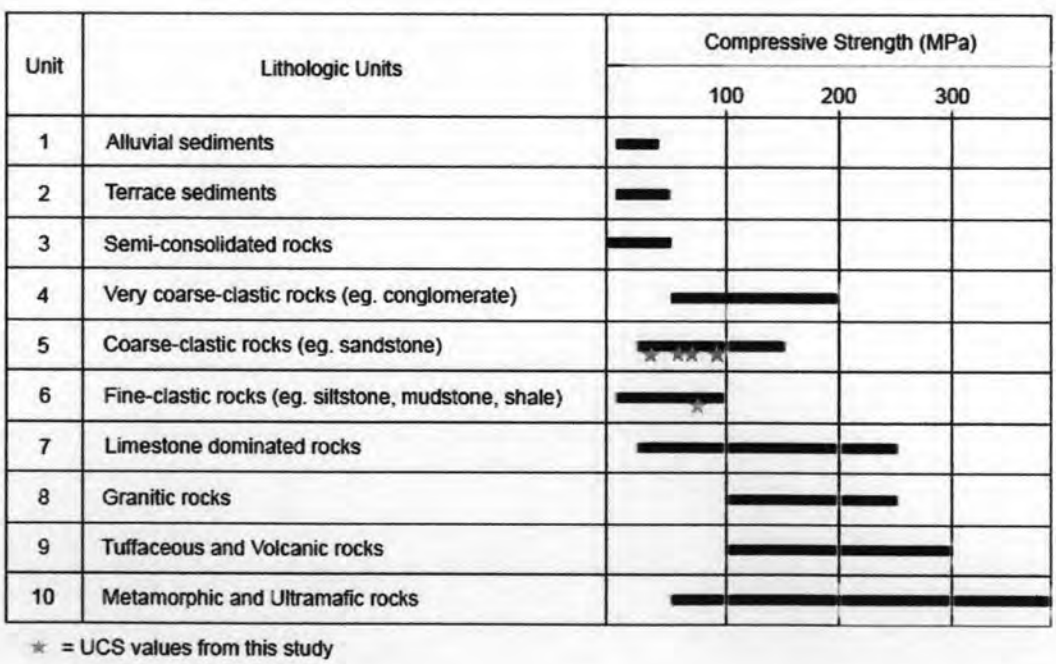

Figure 4.12 Classification of lithologic units based on unconfined compressive strength (UCS) value (modified from Attewell & Farmer, 1976; Roh and Reinhorn, 2008).

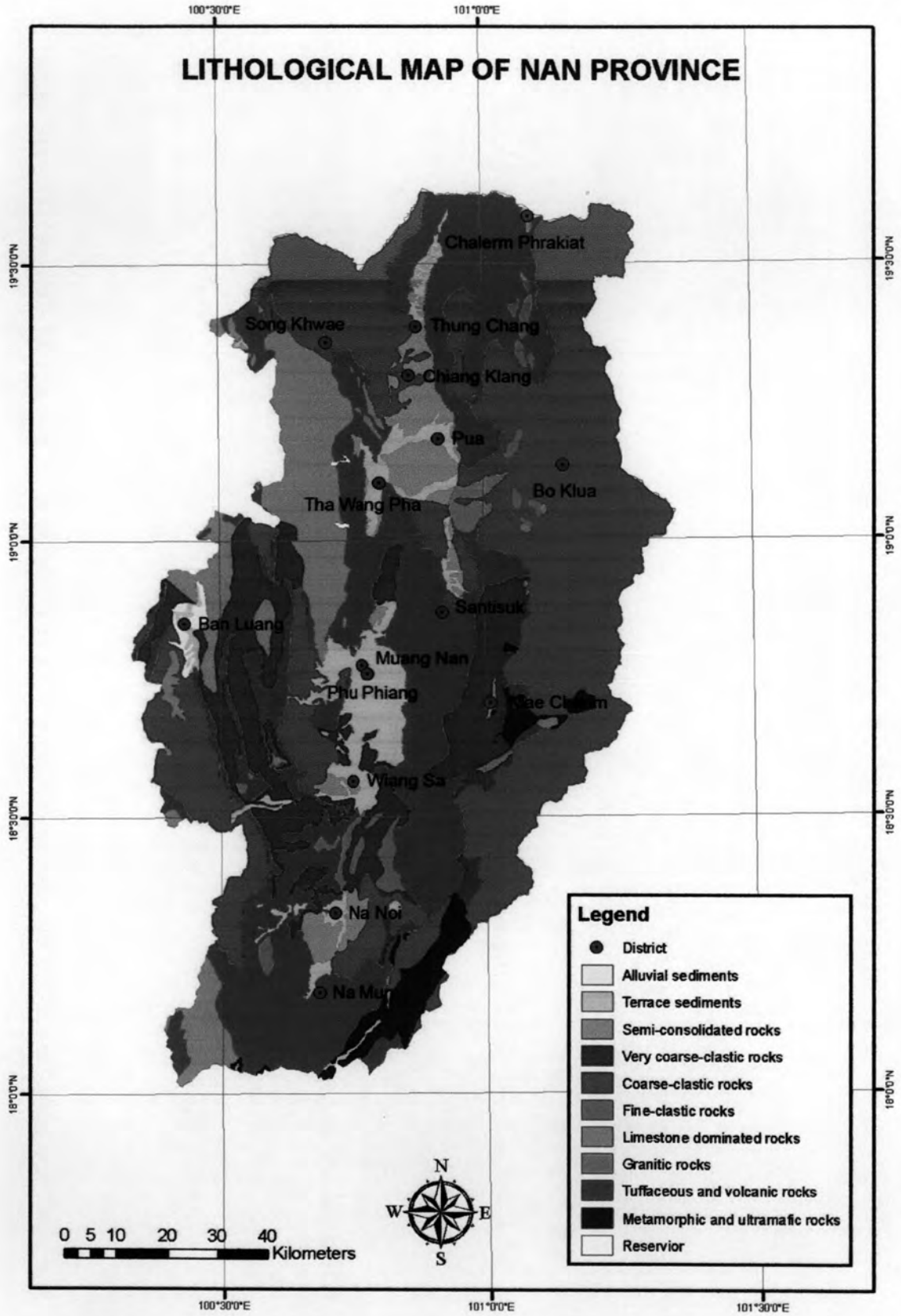

Figure 4.13 Lithological map of the Nan study area modified after geological maps of DMR, rock strength classification and the present fieldwork.

Lineament map: The term lineament represents straight or slightly curved feature, or alignment of discontinuous features, apparent on photographs, images or maps (AGI, 2003). The size of lineaments is related to the scale of photographs or imageries used apart from the lithological information started in the previous section, structural information is very important for landslide hazard assessment. Orientations of discontinuities in the weathered rocks in relation with slope angles and direction are of large influence in the susceptibility to landslides. There are 2 kinds of lineaments namely long lineaments (>3km) and short lineaments (<3 km). The short lineaments are much more common. It is interesting that the short lineaments are quite abundant in area to the northeast of the Nan basin and to the south of Pua Basin. As shown in the fracture map of the Nan study area (Figure 4.14a) that some of the active faults are fault-bounded, and they are longer than the older fault in the pre-Cenozoic solid-rock areas.

In the present study, lineaments were identified from landsat image using contrast stretching with a 99 percent and 3x3 edge filter kernel enhancement can increase the contrast and the clearness of lineaments. Then, lineaments were interpreted by visual interpretation on the computer screen, as mentioned in section 3.2. The straight or slightly curved features or alignments of discontinuous features, apparent on the images were mapped as lineaments as shown in lineament map (see Figure 4.14). They correspond to various types of geological features including fractures (faults and joints), bedding, dykes/veins and some lithological contacts, as well as to spurious man-made feature such as roads, power lines, etc. In relation to landslides, fracture-related lineaments are significant in controlling the locations and forms of landslides. In this thesis, there are two types of lineaments maps of the Nan study area. One is the map of lineaments interpreted from remote sensing data (Figure 4.14a) and the other is the map of active faults (Khaowiset, 2007) and DMR major faults / fractures (Figure 4.14b). Figure 4.14c shows the combination of 2 data maps. This resultant map (Figure 4.14c) was subsequently entered to GIS as a raster format using ArcView software. The buffer command is used to prepare ten separated lineament buffer maps having distance 100 m,

200 m, 300 m, 400 m, 500 m, 600 m, 700 m, 800 m, 900 m, and 1,000 m, and having the 10 different distance zones (Figure 4.15).

As illustrated in Table A2, it is found that the distance from lineaments is within 300 meters covering more than half of the total Nan study area. It is possible to conclude that the more concerned areas located far away from the lineaments, the less landslides possibly occurred.

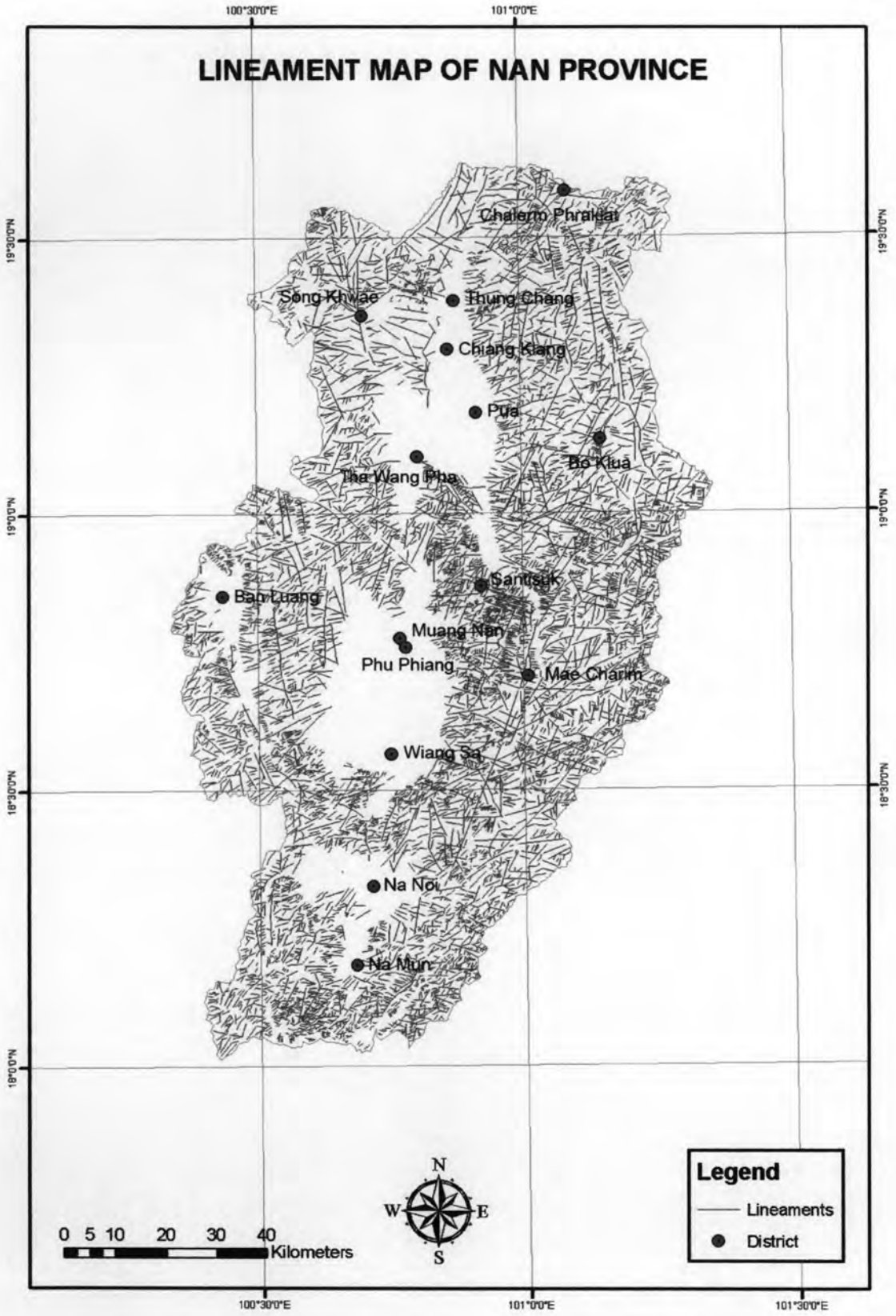

Figure 4.14a Lineament map showing linear structures of the Nan study area, interpreted from Landsat image.

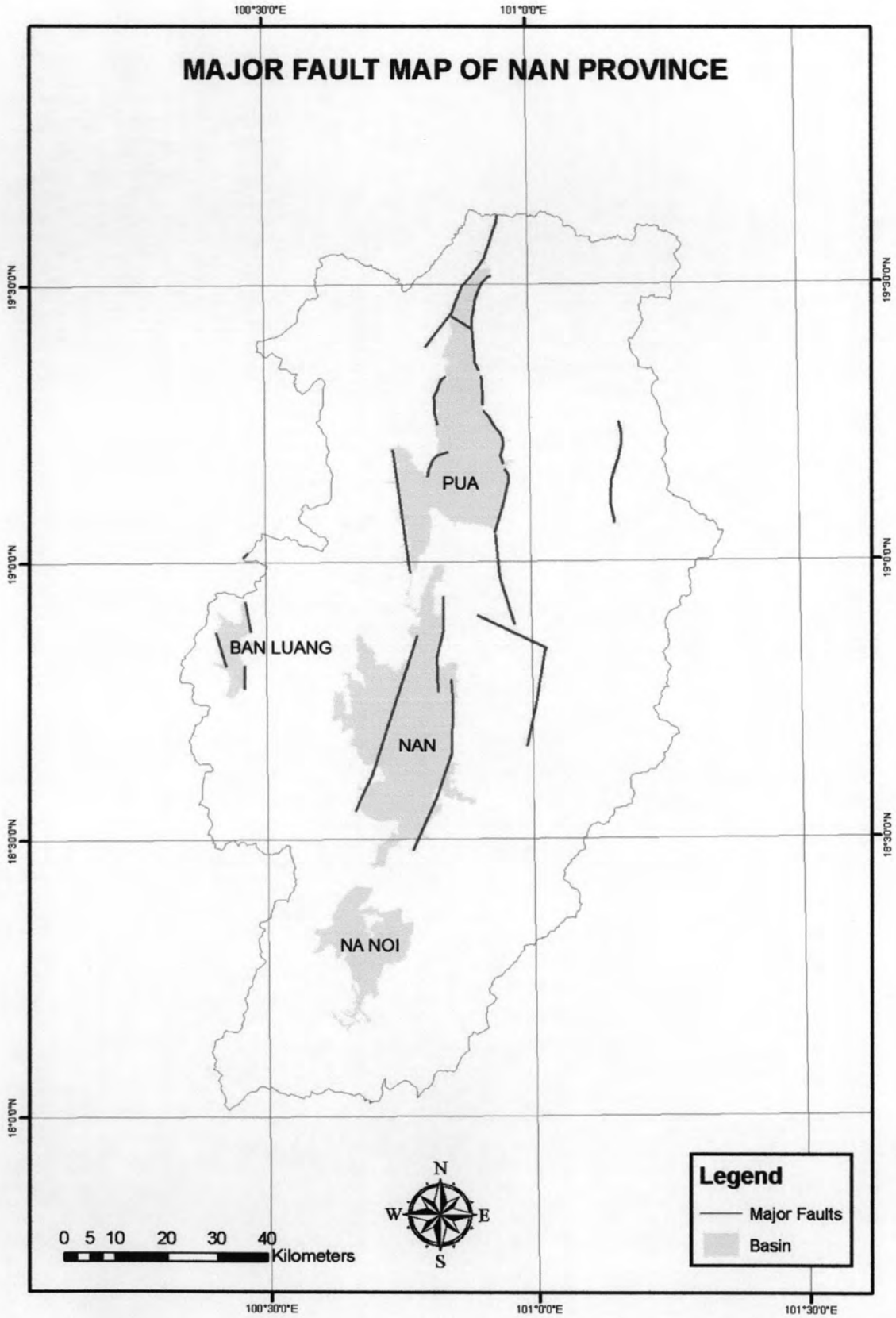

Figure 4.14b Lineament map of the Nan study area shows major faults and fractures based on DMR (2004) and Khaowiset (2007).

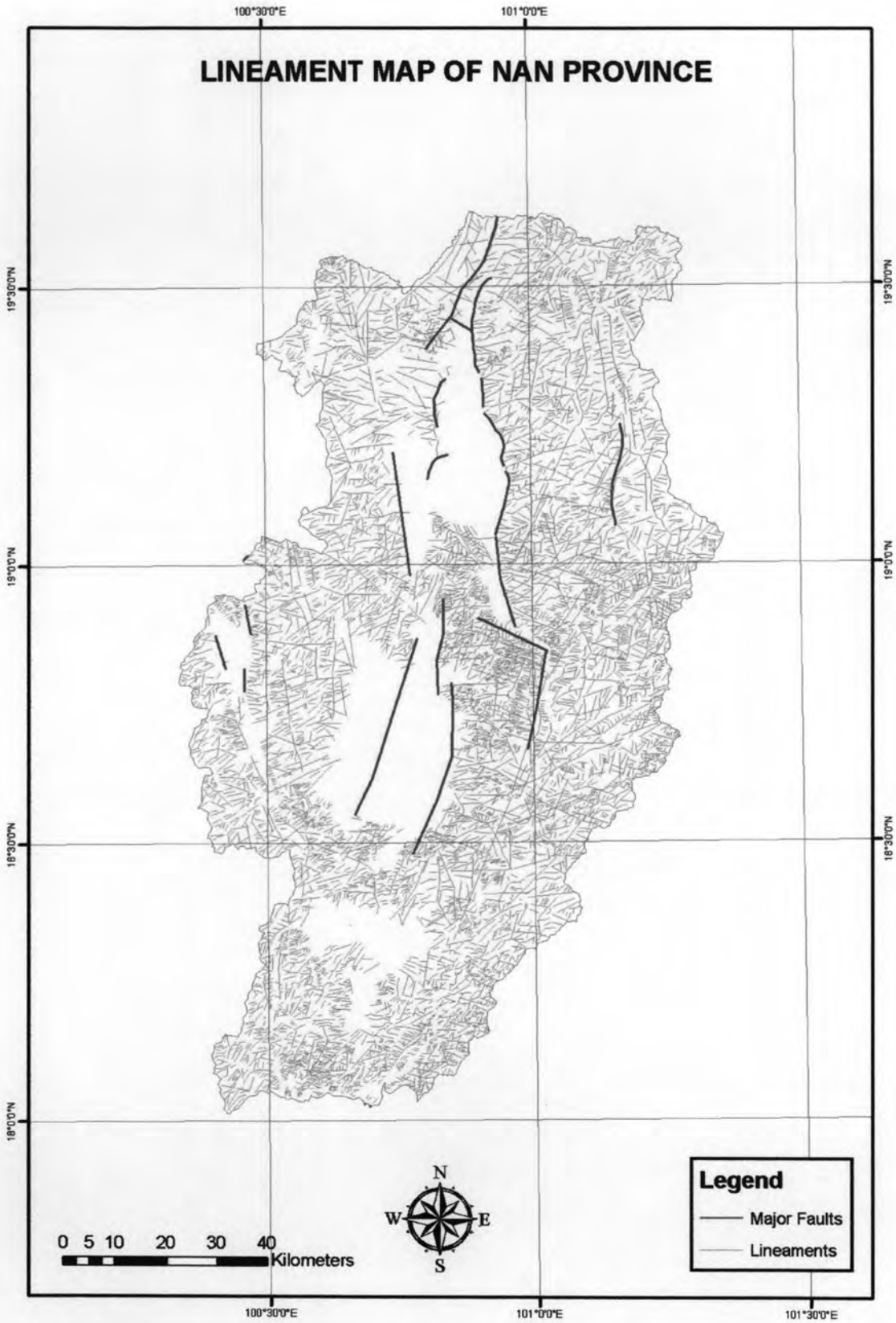

Figure 4.14c Lineament map of the Nan study area shows resultant combination of major faults and lineament.

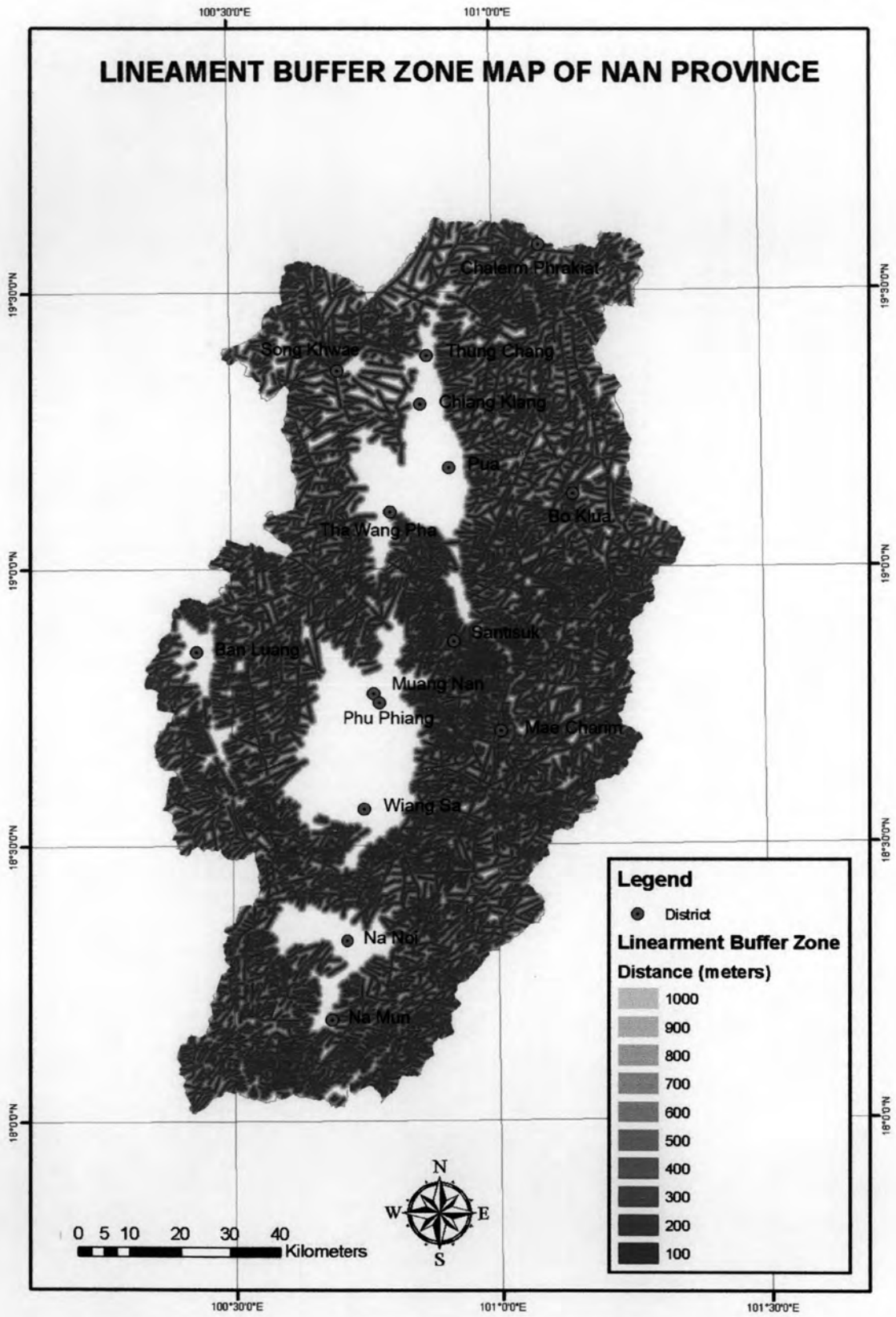

Figure 4.15 Lineament buffer-zone map of the Nan study area showing 10 classes of buffer zones with 100 meters interval.

Land use / land cover map: Basically a land use or land cover map is constructed on a routine basis from medium resolution satellite imaging, which in the case of this study is Landsat data. Typically this is performed by the spectral analysis of individual pixels and their association with other neighboring pixels. The results of classification depend largely on the slopes / types of area, land use type, land cover type, and image acquisition date. However, the results of the classification are directly affected by spectral confusion of land use / land cover types and mixed pixels. The vegetation and soil moisture conditions produce distinctive spectral responses in the electromagnetic spectrum that give the opportunity to the classifier to classify them easily. As a landslide hazard assessment does not only depend on the production of landslide inventory map and its analysis, a complete hazard assessment system requires also the assessment of external factors leading to instability rather than the topography and material derived properties. The land use / land cover distribution is one of the external factors that can easily be mapped and monitored in time if needed with the aid of satellite images (Soesters and Van Westen, 1996). In landslide hazard assessment projects and in environmental and engineering studies, accurate and up to date information about land use / land cover on the regional scale often resembles vital information to help for decision rule generation.

The land use data of the Nan study area provided by Land Development Department (LDD, 2004) are used in this present study as preliminary data. Originally, there are about 6 units as shown in Figure 4.16a and Table A3. Then, for the landslide assessment, they are reclassified and regrouped in to 6 units using the criteria proposed by Townshend (1984). Field observation was also performed for checking the regrouped six classes. They are crop and orchard, teak plantation, open forest, deforestation area, wasteland, and reservoir. The resulting map of land use / land cover is displayed in Figure 4.16b.

Calculation based on Arcview GIS as shown in table 3A in appendix that indicates the land use unit which is the most common is crop and orchard unit which

covers the area of about 30%. Open forest unit ranks second for the land cover in the Nan study area.

As displayed in Figure 4.16b, there are more deforestation areas than the open forest in the Nan study area. Based on GIS calculation shown in Table A3 in Appendix A, it is quite clear that the deforestation area is about 32% of the total mapped area whereas the open forest is about 23%.

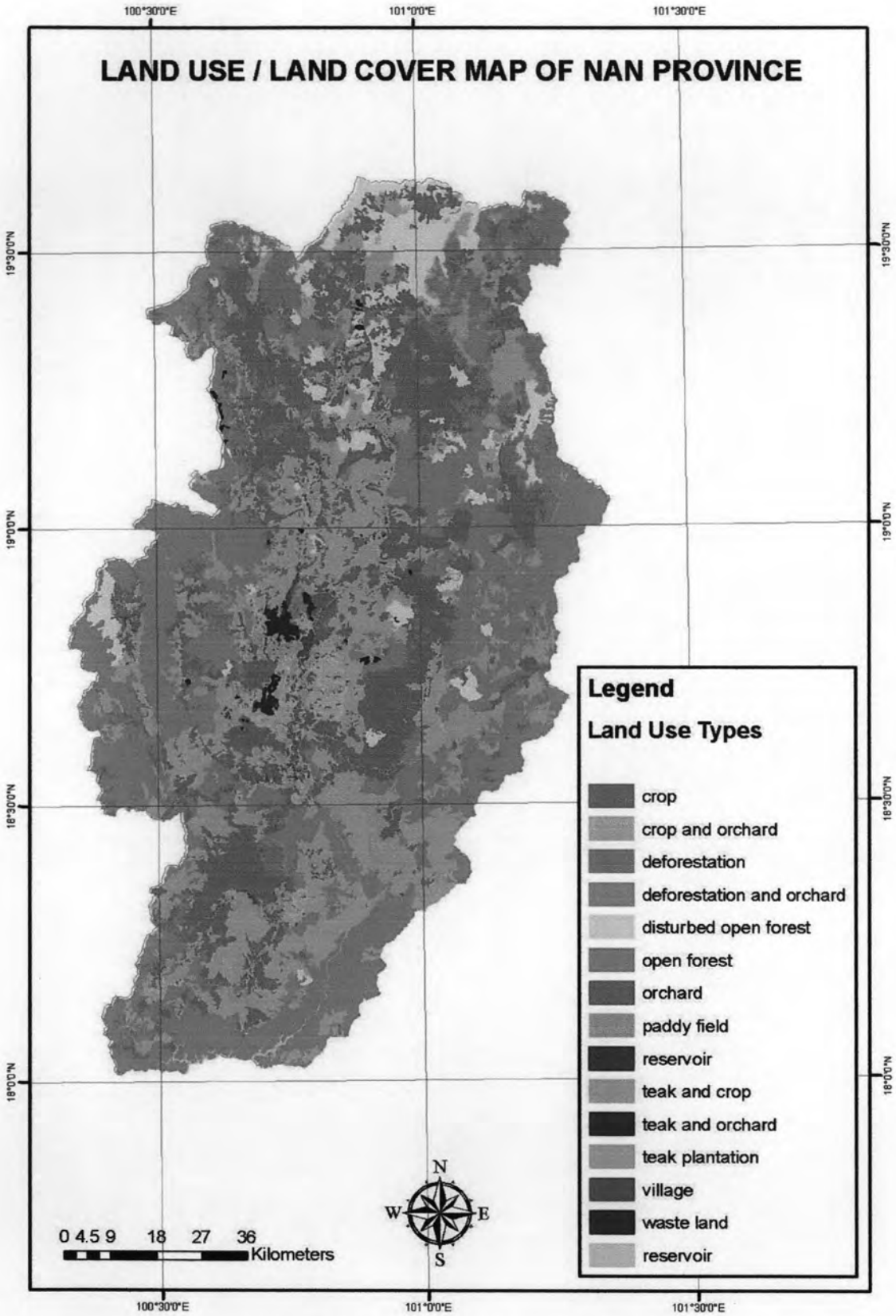

Figure 4.16a Landuse map of the Nan area of study by Land Development Department (LDD, 2004).

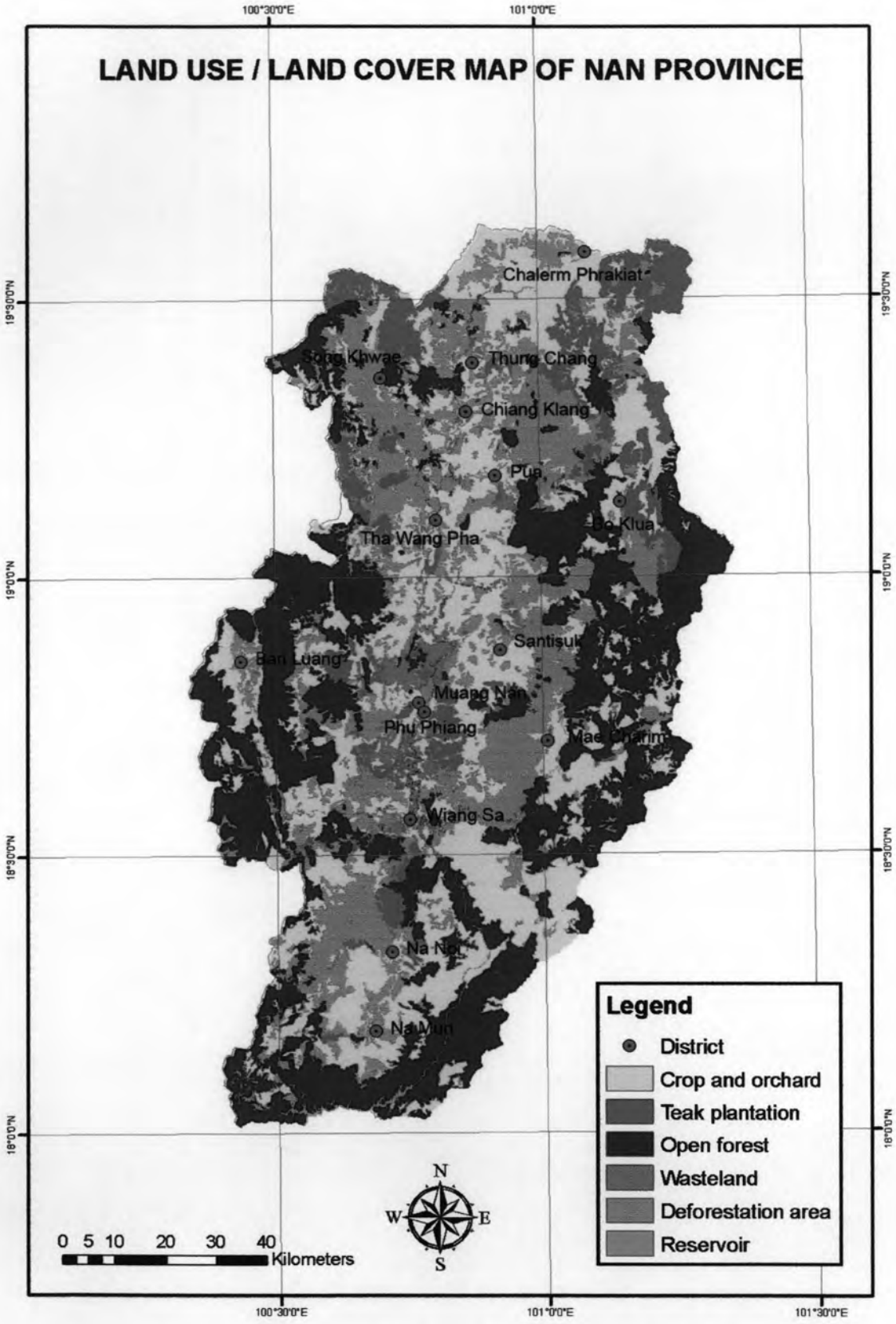

Figure 4.16b Land use / land cover reclassify map of the Nan study area showing distribution of landuses simplified and modified from LDD, 2004).

Elevation map: In this study, digital elevation data was generated from Aster stereo pair of VNIR 3N and VNIR 3B-level 1B (20m contour interval). ENVI 4.1 Aster DTM function is used to process Aster image, while minimum and maximum elevations are given from topographic map. Instead of using a discrete elevation map such as contour lines, it is more advantageous to work with a continuous map. Regarding this advantage, the contour data was converted into a Digital Elevation Model (DEM). This data consists of contour lines and points with elevation information conducted in ArcView format. DEM data can be used to generating contours as an elevation map, slope aspect, slope angle and flow direction. Therefore, DEM data is an essential role for landslide assessment. The result of elevation map (Figure 4.17) show that the Nan province has the elevation ranging from 50 metres to 2,060 meters and was divided into 21 classes of elevation. As shown in Figure 4.17 and Table A4 in Appendix A, it is clear that the high elevation areas of Nan province are those situated to the east of Thung Chang, Chiang Klang, Pua and Santisuk districts.

The result based on GIS calculation indicates that in the Nan study area, the elevation ranges from 200 – 700 meters cover about 70% of the total area. The elevation varying from 300 to 400 meters ranks first in group of elevation in the study area. As indicated in Figure 4.17, the high elevation range is located in the eastern part of Thung Chang, Chiang Klang and Pua districts.

The topographical modeling of the study area also serves as an input to calculate the topographic derivatives such as slope angle and slope aspect maps. These topographic derivatives are very crucial and contain vital information for the flow development in the study area.

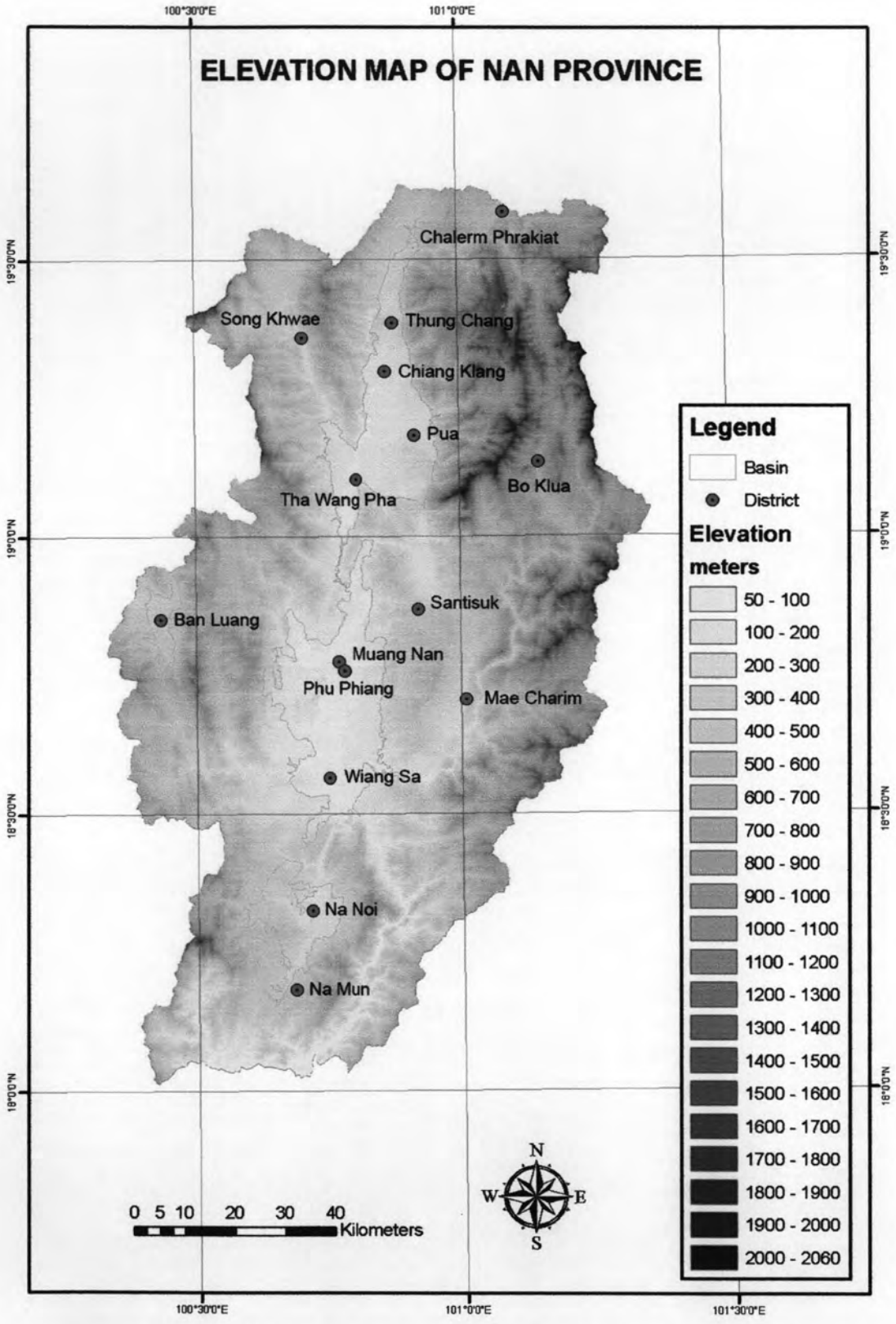

Figure 4.17 Elevation map with 100 meters interval of the Nan study area based on DEM and derived from Aster data. Note that the image data was taken on November 2, 2000.

Slope angle map: Slope measures the rate of change of elevation in the direction of steepest descent. It is widely accepted that slope has a great influence on the susceptibility of a slope to landsliding. Slope instability is normally expected to increase with increase in steepness and slope length. For example, on a flat surface rain drops splash soil particles randomly in all directions and on sloping ground more soils are splashed down slope than up slope. Therefore, a specific terrain is divided into small facets of varying slope angles. In this study, DEM data were used for constructing the slope map of the Nan study area with slope angle values ranging from 0° to 90°. Figure 4.18 and Table A5 in Appendix A shows the slope angle map of the Nan area under study and 9 classes of slope angles were made with the interval of 10°.

The result indicated that the eastern parts of the Nan study area, particularly those in Pua, Thung Chang, and Tha Wang Pha Districts in the Pua Basin, seem to have the highest slope angle. Additionally Bo Klua District is located within and surrounded by slope-angle area.

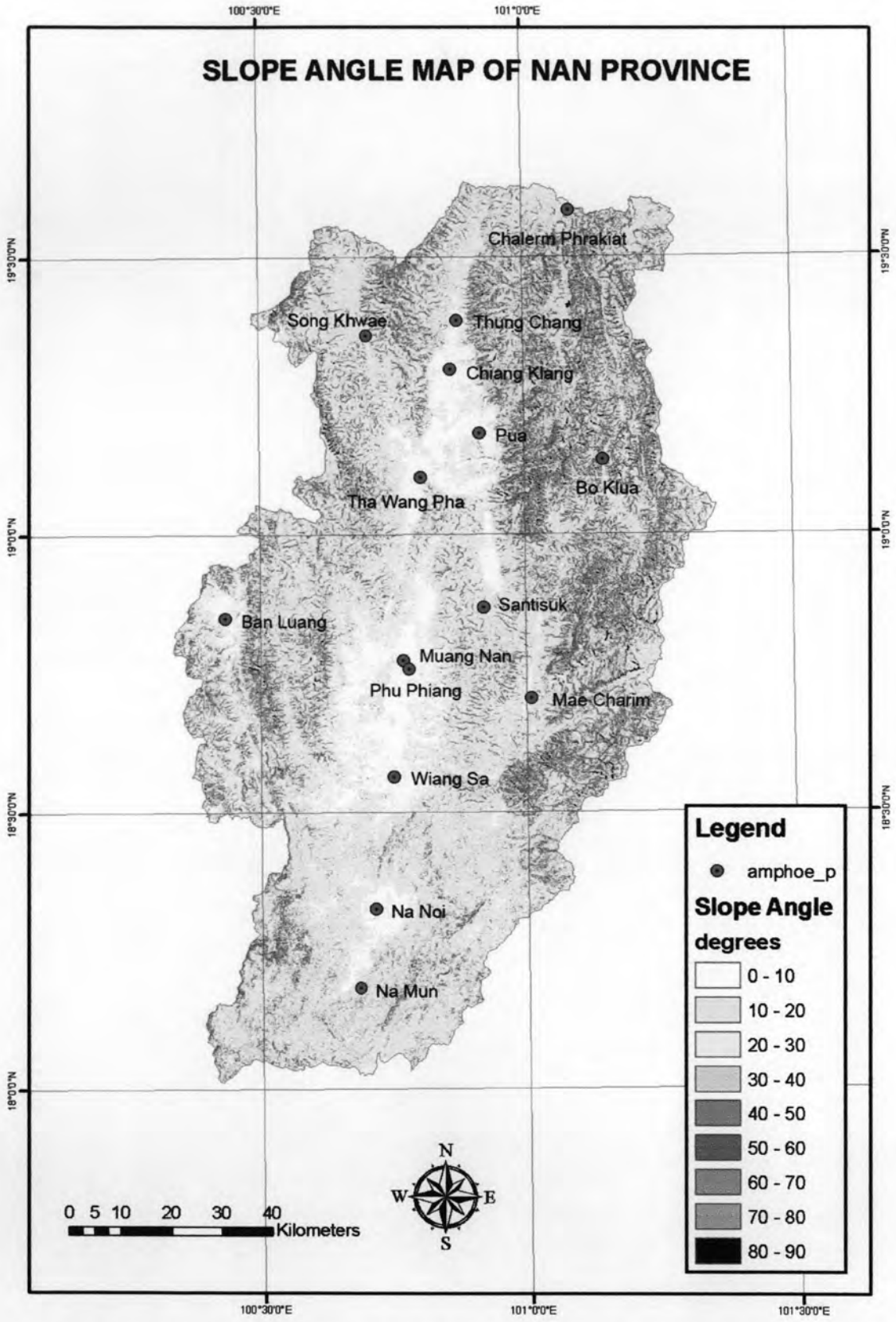

Figure 4.18 Slope angle map of the Nan study area based on DEM data derived from Aster image. Note that the image data was taken on November 2, 2000.

Slope aspect map: Slope aspects (dip direction of slope) are measured in degrees of azimuth from 0 to 360 degrees. The slope aspect is described in terms of 8 cardinal directions, e.g., north, northeast, and east. Each cardinal direction is defined by a set of azimuth values. For instance, slope facing the northeast can have an azimuth reading ranging from 22.5 to 67.5 degrees. The slope aspect always plays a significant role in the analysis of slope stability processes. It was recommended to be used as the input factors for statistical hazard analysis (Van Westen et al., 2008). However, a great care has to be taken for the uses of slope and aspect maps derived from DEM with different resolution (Zhou and Liu, 2004). The direction of a slope faces can be used as an indirect indicator of hydrologic factors. The direction in which a slope face exposed to sunlight has more influence to landslide than other direction of slope. Due to the sunlight, the moisture present in the slope gets dry, and then there is less chance for growing vegetation. So the low vegetation areas on the mountainous slope may have a chance of landslides. In addition, the orientation of a slope face to the prevailing wind is an important in the triggering of landslide. Most of the landslide incidents occur on slope facing to the wind direction.

In the Nan study area, the slope aspect map was also derived from the DEM data and classified into 8 classes as shown Figure 4.19. The result from GIS calculation indicates that the much more common slope aspects are south, southeast and southwest and seem to be located to the east of the study area. Table A6 in Appendix A also confirms the spatial distribution of slopes and the aspect units of three directions attain up to 50% of the total study area in Nan. The average value, which is taken to divide the aspect, is 22.5 degrees.

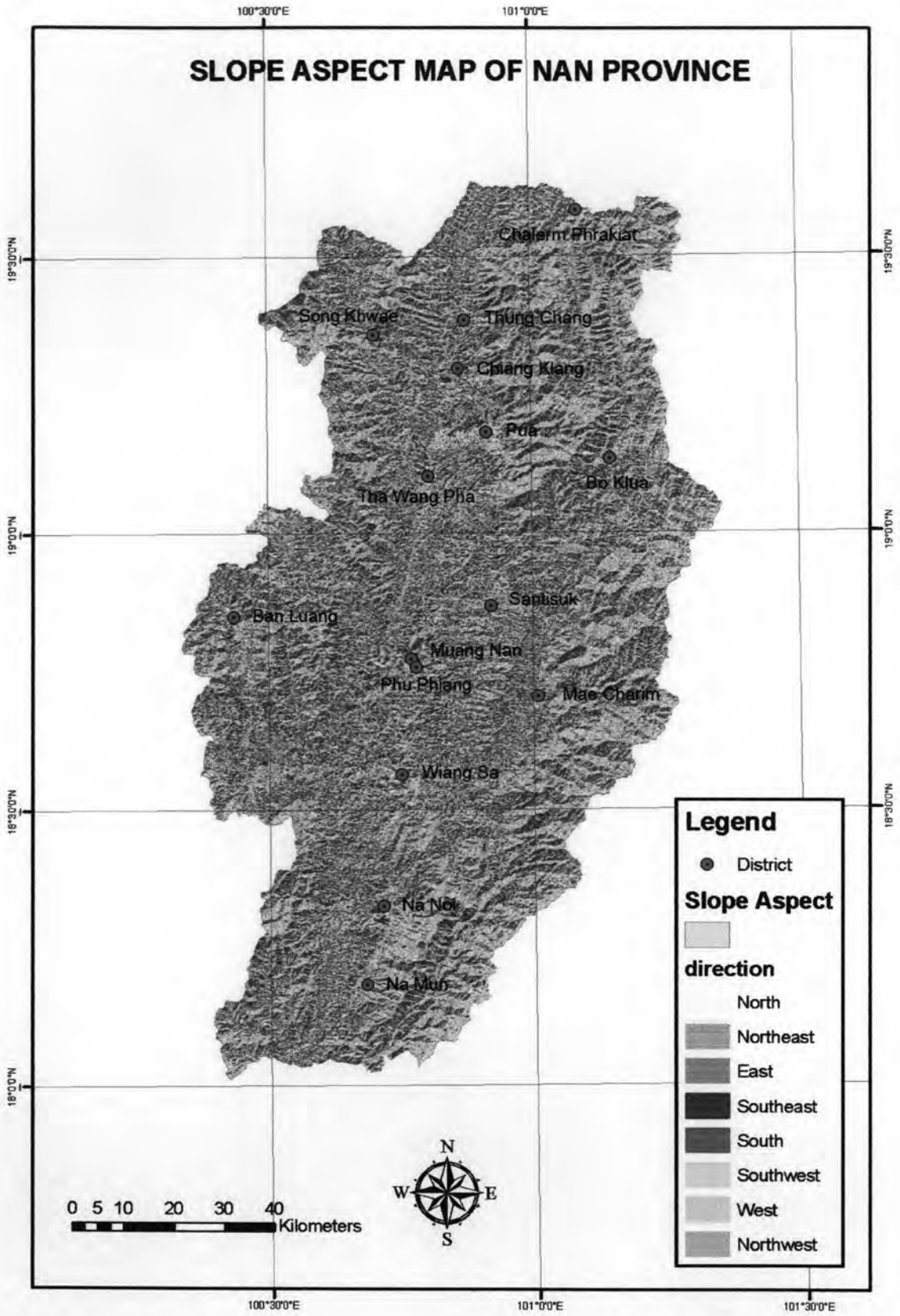

Figure 4.19 Slope aspect map of the Nan study area based on DEM data derived from Aster image. Note that the image data was taken on November 2, 2000.

Flow direction map: A watershed can be described with respect to the surface runoff. The surface runoff was produced inside the watershed and moves to a single watershed outlet. Information regarding the flow direction is recorded as an attribute of each spatial unit within the watershed to represent the flow direction. In this study, a 3x3 moving window is used over the flow direction of each cell. The steepest descent direction from the center cell of the window to one of its eighth neighbors was chosen as the flow path or flow direction. The flow direction factor has a great influence on a transportation of landslide and area can be used successfully in hydrological modeling of the hazard assessment (Soeters and Van Westen, 1996). Figure 4.20 provides 8 classes of the flow directions in a raster format of ArcView. It is shown that the most prominent direction of flow direction is in the south to southeast direction. The eastern part of Pua Basin has a distinct flow direction. This direction covers the area of about 15% of the total Nan study area, as displayed in Table A7 in the Appendix.

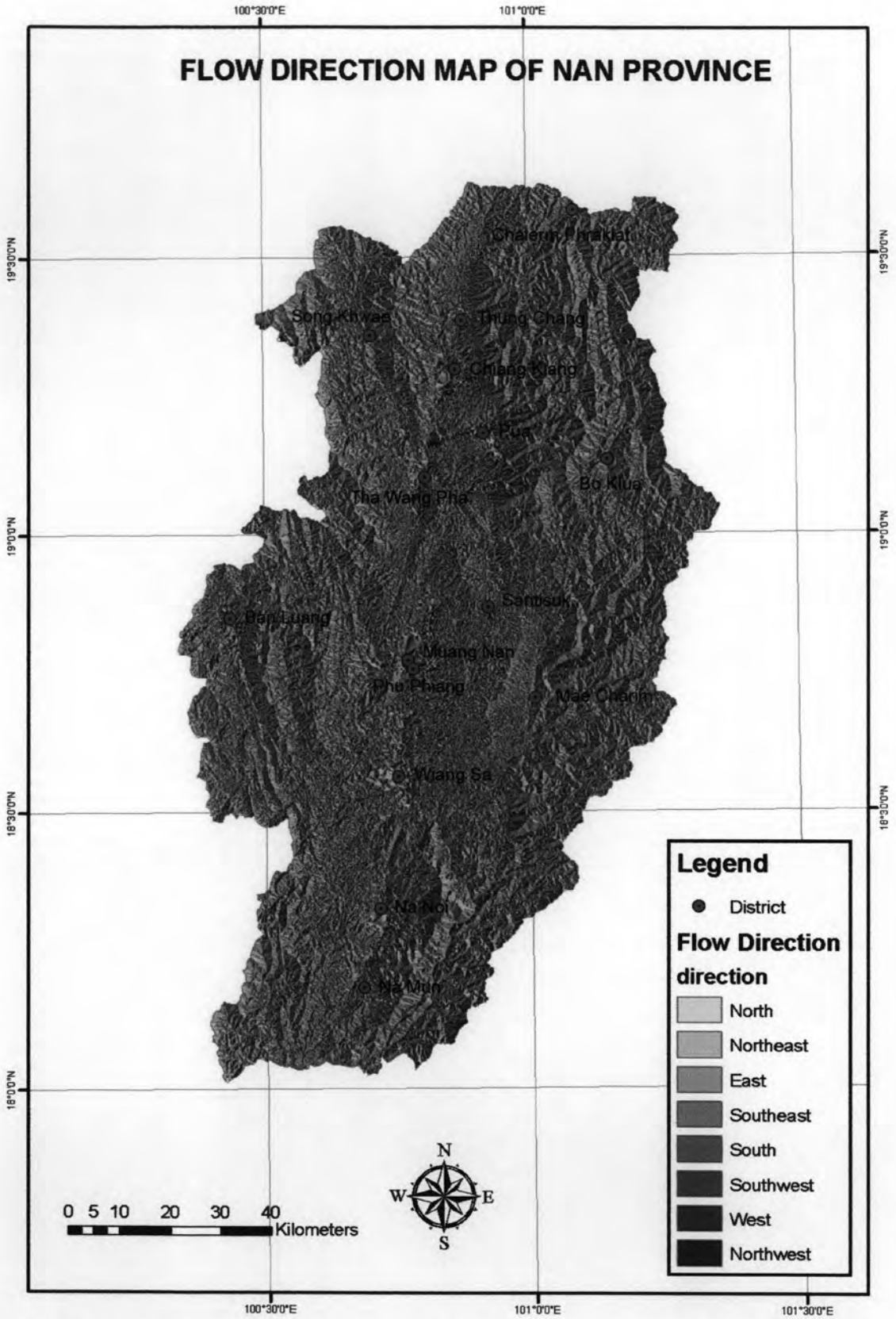

Figure 4.20 Flow direction map of the Nan area of study based on DEM data derived from Aster image. Note that the Aster image was taken on November 2, 2000.

Normalized Difference Vegetation Index (NDVI) map: The vegetation index represents the plant-cover condition and ranges from minus one to one. When the land is naked, the NDVI value tends to be minus one, and when the land is covered with full vegetation, the NDVI approaches one. The NDVI varies with the vegetation type, the seasonal change, and the percentage of the vegetation cover surface. NDVI map was obtained from Landsat 7 ETM satellite image and computes in ENVI 4.1 software as shown in equation (4.1).

$$NDVI = (IR - R) / (IR + R) \quad (4.1)$$

Where IR is the infrared radiation value and R is the red light radiation value. NDVI is calculated on a pixel base. The result of NDVI calculation can be divided in to 8 classes ranging from -1 to 1 as shown in Figure 4.21. The result shows that less vegetation covers occur in most Cenozoic basin whereas the area covered with vegetation is located in the high mountainous areas. Table A8 in the Appendix A shows that more than 70% of the total area covers, to some extent, with the vegetation.

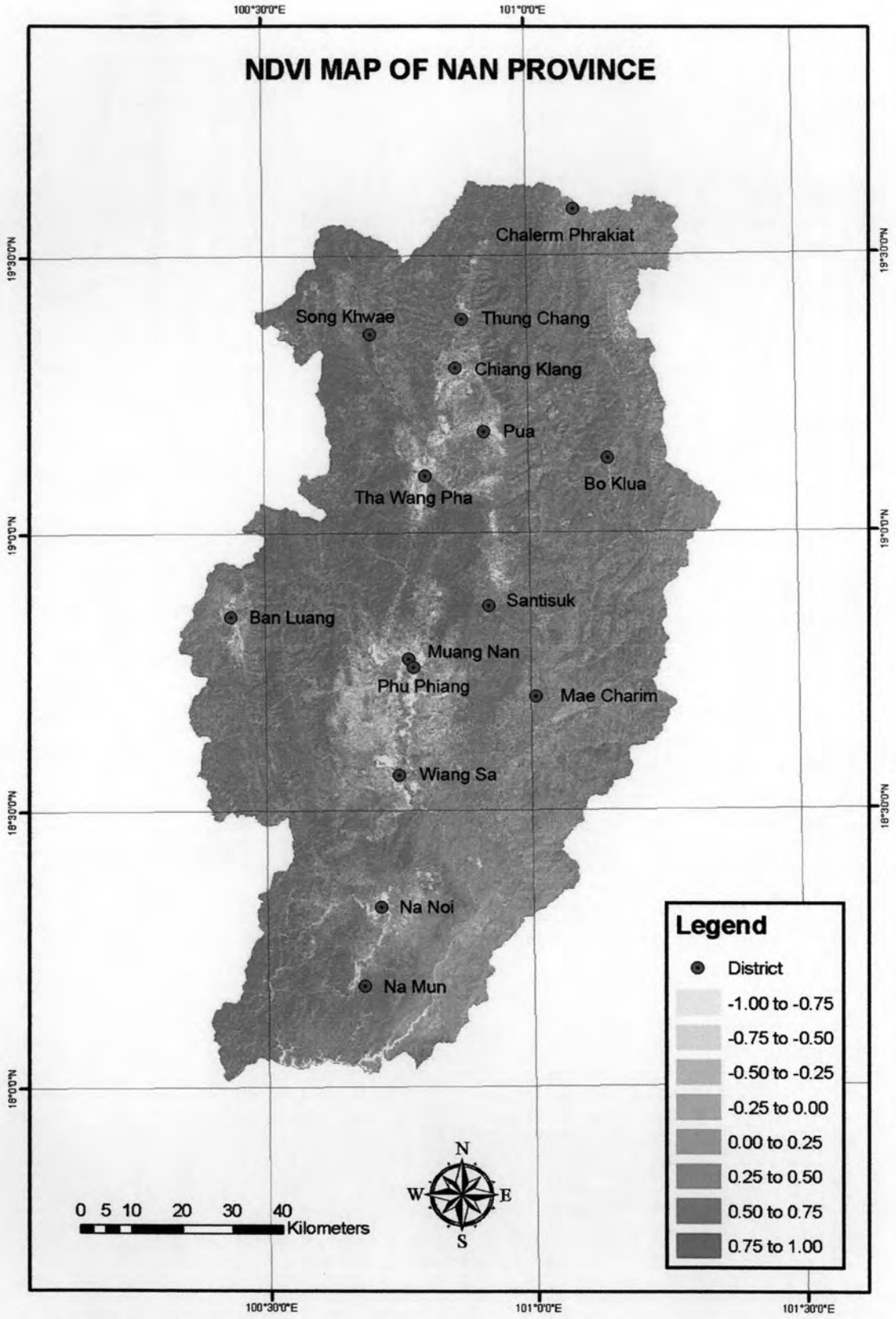

Figure 4.21 Normalized vegetation index (NDVI) map of the Nan study area based on Landsat image using ENVI program.

4.2 Results Related to Landslide Assessment Analyses

The probability analysis and weighting for landslide occurrence on the factor maps were calculated from the result of landslide assessment analyses. The probability analysis comprises the analyses of the relationship between landslide occurrences and factor maps, and the calculation of probability ratio, which is explained as follows:

4.2.1 Relationship between Landslide Occurrence and the Factors

Relationship between landslide occurrence and the factors relies very much on examining the spatial relationships between interpreted landslide scars and individual factors. The method applied is to cross-tabulate the past landslide location map with each factor map. Then, a landslide distribution table is developed and it indicates the number of landslide location occurring on each specific area of attribute of each factor (e.g. each lithology attribute of the lithologic layer). The results of the relationship between landslide scars or occurrences and the factors are presented in the Appendix A (Tables A1 to A8). They allow important deduction to the role and possible significance of factors, as discussed below:

Landslide occurrence on lithology factor: As shown in Table A1 in Appendix A, landslide occurrence value is very high in the coarse-clastic sedimentary rocks, including sandstone, sandstone interbedded with siltstone. It attains up to more than 54% points of landslides in the Nan study area. The value is also high in tuffaceous / volcanic rocks (22%) and limestone-dominated rocks (12%) and granitic rocks. It is low to very low for landslide occurrence (3-5%) on the metamorphic and ultramafic rocks, metasedimentary rocks, semi-consolidated rocks, alluvial and terrace deposits. Therefore, based on the lithology alone, it is quite likely that the presence of highly-fractured and weathered sandstone interbedded with other sedimentary rocks is the cause of landslide occurrence. The additional failure also occurs along bedding planes of interbedded rocks.

Landslide occurrence on the buffered lineament factor: L andslide occurrence on the buffered lineament is shown in Table A2 in Appendix A. Most of landslide occurrences was occurred in the first (<100 m) and second (100 - 200 m) order of buffered lineament zone, which shows an increasing of the landslide affected area in the proximal distance to lineaments. The landslide occurrence is gradually decreased with increasing distance from lineaments because lineaments are believed to act as a week zone of bedrocks. The degree of landslide occurrence on 0 - 100 and 100 – 200 meters buffer of lineaments is very high. Totally about 50% points of landslide. The high landslide hazard occurrence is on 200 - 300, 300 – 400 and 400 – 500 meters away from lineaments. Low to very low landslide occurrences are on the distance of 500 – 1,000 meters from lineaments.

Landslide occurrence on land use / land cover factor: The trend of landslide occurrence on the land use / land cover based on the LDD data is shown in Table A3 in Appendix A. From the analysis, the landslide occurrences total up to 60% points of landslides are higher on the teak plantation area, open forest and deforestation areas than other land use area. The landslide occurrences are very high on densely open forest and deforestation areas, and high on the teak plantation land use area. The observed landslide occurrences on the other land use types are low to very low. The reason is simply because the landslides frequently occurred on steeply-slope and mountainous areas dominated with deforestation and open forest areas.

Landslide occurrence on elevation factor: Percent points of landslide occurrence on the elevation are shown in Table A4 in Appendix A. The maximum points of landslides occurred in the area with the rank of elevation between 400 – 500 meters. The trend of landslide almost up to 60% is highly occurred at elevation ranging from 300 – 700 meters. This elevation range is generally located in the high steep slope

mountainous area. As shown in Figure 4.17, it is likely that these areas are situated to the east of the Pua basin.

Landslide occurrence on slope angle factor: From Table A5, it is found that the landslide occurrences within the slopes ranging from 10 – 30 degrees are relatively high (totally up to 60%). The trend of landslide occurrence in Table A5 shows that the landslide occurrence is slightly decreasing with the steeper slope, and is decreased when the slopes are higher than 40 degrees. This can be explained that the steep slope of higher than 40 degrees is relative stable due to the exposure of the hard and unfractured bedrock.

Landslide occurrence on slope aspect factor: The tendency of landslide occurrence as given in the Table A6 in Appendix A denotes that areas of the south and southeast slope aspects have been relatively highly affected by the 22.47 and 19.71 percent points of landslide location number, respectively. The analysis based on the GIS calculation, indicates that the north and northeast slope aspects are less affected by landslide occurrences. The result is related to the wind direction of the rain-storm. It is considered from this analysis that the landslides occurred in August, 2006 disaster was induced by southwestern monsoon.

Landslide occurrence on flow direction factor of a watershed: Landslide occurrence on flow direction is tends to be high in east to southeast direction (up to 20% points of landslides (Table A7 in Appedix A). The high percent of landslide occurrence also distributes in southeast to south direction which is slightly more than 15% point. It affects the peak flow rate of a stream and thus initiation of debris flow. The flow direction depends directly on the direction of the steepest slope. Therefore, the surface runoff moved from the highest point to the lowest point. The lowest point is called the watershed outlet, which is eventually indicated by the landslide affected area.

Landslide occurrence on NDVI factor: The relationship between landslide and vegetation index is shown in Table A8 in Appendix A, Landslide occurrences is tend to be high on the vegetation index values between 0.25 and 1.00 which is indicate the dense vegetation areas and It is also shown based on GIS calculation that the NDVI is moderate on the vegetation index value -0.50 to 0.25, suggesting slightly to moderately vegetation areas. The observed landslide occurrences on the other NDVI values are low to very low, which are mostly less than 5% point of landslides. The landslide occurrence on vegetation index is conformed with the landslide occurrence on land use / land cover.

4.2.2 Probability Analysis

The probability analysis is performed herein in term of the probability ratio. The probability ratio of landslide occurrence in each factor's classes can be calculated with ArcView GIS from percentage of landslide occurrences d ivided by percentage of total area of the same attribute of the factor from the result on Tables A1 to A8 (cf. equation 3.1). The probability ratio is used as a guide to where further landslides are likely occurring. The probability ratio of landslide occurrences on unit that equals or is higher than 1.00 will be rank and used for reliability probability weighting analysis but the probability of landslide occurrence on unit lower than 1.00 will not be included in ranking. The results of probability ratio of each factor's classes are shown in Appendix B (Tables B1 to B8) and discussed below:

Probability ratio of landslide occurrence on lithology: As discussed in the previous section that the percentage of landslide locations and percentage of landslide affected areas for the coarse-clastic sedimentary rock unit is the highest as compared to the other classes. The landslide probability ratio of the medium-clastic sedimentary rock unit is the highest (probability ratio = 1.49) as observed from the Table B1 in Appendix B. The next of rank is the limestone-dominated rock unit (probability

ratio = 1.47) and the tuffaceous and volcanic rock unit rock unit (probability ratio = 1.00) is the last of rank. Based on GIS calculation, the percentage of landslide affected areas of the tuffaceous and volcanic rock unit is very low less than 0.6 percent of the whole Nan area. In this case, the landslide probability ratio denotes the value of likelihood landslide occurrence in the class compared with its area.

Probability ratio of landslide occurrence on buffered lineament: In this case, the distance from lineament of about 0 – 100 meters (about 1.3% probability ratio, PR) has the highest probability ratio of landslide occurrences as shown in Table B2 in Appendix B which indicates that this lineament range has a very high hazard for the occurrence of landslides (Table B2).The high hazard is represented by the range of distance from 100 to 600 meters from lineaments which is more than 1% PR (probability ratio of 100 – 200 meters = 1.19, probability ratio of 300 – 400 meters = 1.14, probability ratio of 400 – 500 meters = 1.11, probability ratio of 500 – 600 meters = 1.03, probability ratio of 200 – 300 meters = 1.01).

Probability ratio of landslide occurrence on land use / land cover: Table B3 in Appendix B indicates that the landslide probability ratio in the wasteland area of the landslide is the highest value up to 1.8. However, the percentages of landslides affected area of the wasteland area is very low (2.9 percent of the whole area) comparing to those of the other areas and the wasteland area is very low (1.6 percent of the total area) also. The teak plantation and the densely open forest areas of land use has high landslide probability ratio (about 1.7 and 1.3, respectively). This shows the high accuracy of the ArcView GIS calculation as the result conformed with occurrence of landslides based on the field survey.

Probability ratio of landslide occurrence on elevation: From Table B4 in Appendix B, it shows that there are 11 classes of elevation of the Nan area ranging

from 400 to 1,600 meters, which the probability ratio of landslide occurrence are higher than 1.00. Calculation of the probability ratio of landslide occurrence shows that the elevation of the Nan area in the range of 1,500 – 1,600 meters is the highest landslide hazard zone with the probability ratio of 1.8. Other classes are considered to be relatively moderate to high landslide hazard zone with the elevation of 700 – 800 meters (PR = 1.39), 1,000 – 1,100 meters (PR = 1.37), 900 – 1,000 meters (PR = 1.36), 1,200 – 1,300 meters (PR = 1.35), 500 – 600 meters (PR = 1.33), 800 – 900 meters (PR = 1.31), 400 – 500 meters (PR = 1.22), 600 – 700 meters (PR = 1.22), 1,100 – 1,200 meters (PR = 1.20), and 1,300 – 1,400 meters (PR = 1.10), respectively.

Probability ratio of landslide occurrence on slope steepness: The slope is one of the important factors affected the landslides occurrence in the Nan study area, particularly those in the high mountainous area. As shown in Table B5 in Appendix B, the probability value for slope in the range of 10 – 40 degrees is considered to be high for landslide occurrence with the PR =1.21 for the 10° – 20° slope, = 1.18 for the of 20° – 30°, and 1.16 for 30° – 40° slope degrees, respectively. So the areas covered by these slope classes are quite unstable.

Probability ratio of landslide occurrence on slope aspect: Table B6 in Appendix B show that the probability ratio of landslide occurrence for the slope aspect to the south direction is the highest in term of landslide hazard with the probability ratio = 1.65, whereas the southwest and the west are considered to be quite high with the PR of 1.52, 1.05, respectively). It seem landslides possible to occur along the slope area in the southwest aspect direction.

Probability ratio of landslide occurrence on flow direction: As shown in Table B7 in Appendix B, the trend of landslide probability ratio value distributes are in 2 main directions, east and west directions. The probability ratio of flow direction

factor (1.27) is the highest on the southeast to south directions. The high landslide hazard area is composed of northeast to southeast and northwest to southwest directions (probability ratio of E to SE = 1.26, probability ratio of SW to W = 1.22, probability ratio of W to NW = 1.11, probability ratio of NE to E = 1.08, respectively). It is quite interesting that the result of flow direction of the study area conforms to the direction of the slope aspect as shown in Table B6.

Probability ratio of landslide occurrence on NDVI: The probability ratio (1.24) of landslide occurrence on NDVI index values 0.75 to 1.0 is higher than those of the other NDVI index values, as shown in Table B8 in Appendix B. The NDVI index value of 0.5 to 0.75 has the probability ratio of 1.06 and that of -0.25 to 0.00 has the probability ratio of 1.00 are high landslide hazard area. From result that shows in Table 8A, it conforms to the probability of landslide occurrence on land use / land cover factor.

4.2.3 Weighting for the Importance of Factors on Landsliding

The identification of potential landslide areas requires that the factors are considered to be combined in accordance with their relative importance to landslide occurrence. This can be achieved by developing a ranking and weighting scheme in which factors and their classes are assigned with numerical values. The importance of a factor as a predictor of landsliding can be considered in different ways. Two possible approaches were used in this study. These approaches are based on the reliability probability method, and the accountability probability method.

In both performance measures, only probability values of attributes ≥ 1 (i.e. mean and above mean landslide incidence) are considered. The mean landslide incidence value means the probability ratio of landslide occurrence for the whole area (cf. equation 3.2). Then, each single factor is first assigned with a numerical ranking based on the probability ratio of landslide occurrences. The highest probability ratio was

assigned with the first rank of importance. The rank value r_i is between 1 and n, whereas r_i =1 is the rank of highest importance, and n is the number of all factors analyzed. In this study, 8 factors were ranked (n = 8). Weights are also assigned to each factor's rank of both methods (cf. equation 3.6). The larger weight is the greater chance the landslide occurs. Before the weights can be combined, they need to be normalized (cf. equation 3.7).

Weighting for the importance of factors on landsliding were calculated based on reliability probability ratio of each factor as discussed below:

Weighting for the importance of factors on landsliding based on reliability probability ratio: Reliability means the value of factor corresponding to landslide. The reliability probability is calculated as the percentage are a of factors corresponding to landslides. It is computed for each factor (cf. equation 3.4). The results are the reliability probability ratio of each factor (Greenbaum et al., 1995), as a predictor of landsliding as shown in the Appendix C (Tables 1C to 8C).

Reliability probability ratio of each factor is meant the likelihood of landslide occurrence when compared to the probability of landslide occurrence for the whole area. For example, the reliability of lineament is 1.35 that means the chance of landslide occurrence in the area according to lineament factors is 1.35 times of the mean landslide incidence value. Then the results from Tables 1C to 8C were used for ranking and weighting of importance of factors as shown in Table 4.2.

Table 4.2 Overall ranking order and weighting of importance of factors based on reliability probability ratio.

Type of Factors	Reliability	Rank	w	w_i	w_i x100
Lithology	1.50	1	8	0.22	22
Slope Aspect	1.42	2	7	0.20	20
Land use / Land cover	1.40	3	6	0.17	17
Elevation	1.29	4	5	0.14	14
Slope Steepness	1.19	5	4	0.11	11
Flow Direction	1.19	6	3	0.08	8
Lineament	1.17	7	2	0.05	5
NDVI	1.11	8	1	0.03	3
Total		**n=8**	**36**	**1**	**100**

Table 4.3 The importance of factors on landslide occurrences in the Nan study area.

Type of factors	The importance on landslide occurrence	
	Rank	Weight
Lithology	1	22
Slope Aspect	2	20
Land use / Land cover	3	17
Elevation	4	14
Slope Steepness	5	11
Flow Direction	6	8
Lineament	7	5
NDVI	8	3

4.3 Landslide Hazard Zonation Map

The probability ratio map of each factor and their weights are used to produce landslide hazard (zonation) map of the Nan study area as shown in Figure 4.23. The degree of landslide hazard presented herein is considered relative, and represents the expectation of future landslide occurrence based on the conditions of that particular area. Landslide susceptibility is relative to the condition of each specific area, and cannot be assumed to be identical for a different condition area.

In this study, landslide hazard map, or landslide susceptibility (zonation) map, was produced by bivariate and probability weighting models. This landslide hazard map was generated using the formular proposed by Lee (2004) expresses as equation (4.2);

$$LPI = \sum^{j}\sum^{i}\{(F_1 W_1)/100 \quad \text{.....(4.2)}$$

; Whereas: LPI is landslide probability index;

j

F_1 is the data layers of each factor (1,2,3,...j, with j = 8, in this study), which is represented the probability index values (cf. Table 1B-8B). For example, F_1 = Slope factor map contained the probability ratio of landslide occurrence of each slope class; and

i

W_1 is the weight of each factor considered (1,2,3,....i, with i = 8, in this study).

4.3.1. Landslide Hazard Map Based on Reliability Probability Weighting

The spatial data layers representing probability ratio values of the factor's classes were used as input data for spatial analysis in the GIS. The input data layers were multiplied by their corresponding reliability weighted, and were summed up together to obtain the Landslide Probability Index (LPI) for each 30 by 30 metres grid cell as shown in Figure 4.22 is an example of LPI using input data.

The landslide probability index obtained ranges from 0.36 to 1.53. These could be classified into five landslide susceptible classes. A judicious way for this classification is to use the relative equal interval to separate the landslide potential index into 5 landslide hazard classes or levels.

The level of landslide hazard is measured on the ordinal scale based on the equal interval values. Then, five levels of relative hazard are defined on a landslide susceptibility map: (0) = no hazard, (1) = very low, (2) = low, (3) = moderate, (4) = high, and (5) = very high hazard (Table 4.4). The landslide hazard map based on reliability probability weighting are shown in Figure 4.23.

The landslide hazard map shows that almost 4 percent of the whole area lies in the highest landslide prone area. The percentage of very low hazard area is the lowest at 0.24 percent of the total area. The percentage of no hazard area is the highest at close to 20 percent of the total area. Similarly, about 10 percent, 36 percent and 35 percent of areas lie in the low, moderate and high landslide hazard levels, respectively. It is obvious from the result map that the areas under high and very high hazard level are located within the mountainous area in the northern part of the study area.

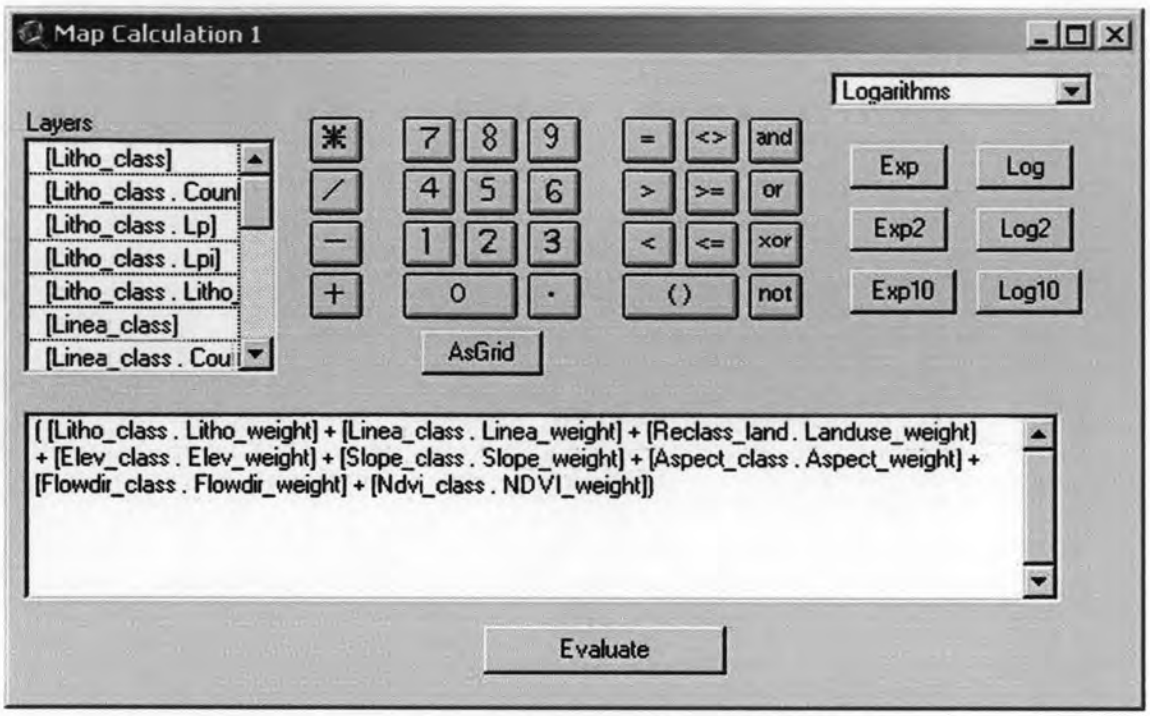

Figure 4.22 Input data layers (lithology, lineaments, landuse, elevation, slope angle, slope aspect, flow direction and NDVI) multiplied by reliability weighted and summed up for values of the Landslide Potential Index (LPI) for each 30m by 30 m (remark: Ndvi_class. NDVI_weight = NDVI unit map layer with probability index of landslide occurrence x reliability weighted of its layer).

Table 4.4 Landslide probability index values and hazard levels of the Nan study area based on reliability probability weighting.

Hazard level classes	Landslide Probability Index	Landslide Hazard Level	% of Area
0	0.00	No Hazard	16.16
1	0.36 – 0.59	Very Low	0.24
2	0.59 – 0.83	Low	9.47
3	0.83 – 1.06	Moderate	35.71
4	1.06 – 1.29	High	34.75
5	1.29 – 1.53	Very High	3.67

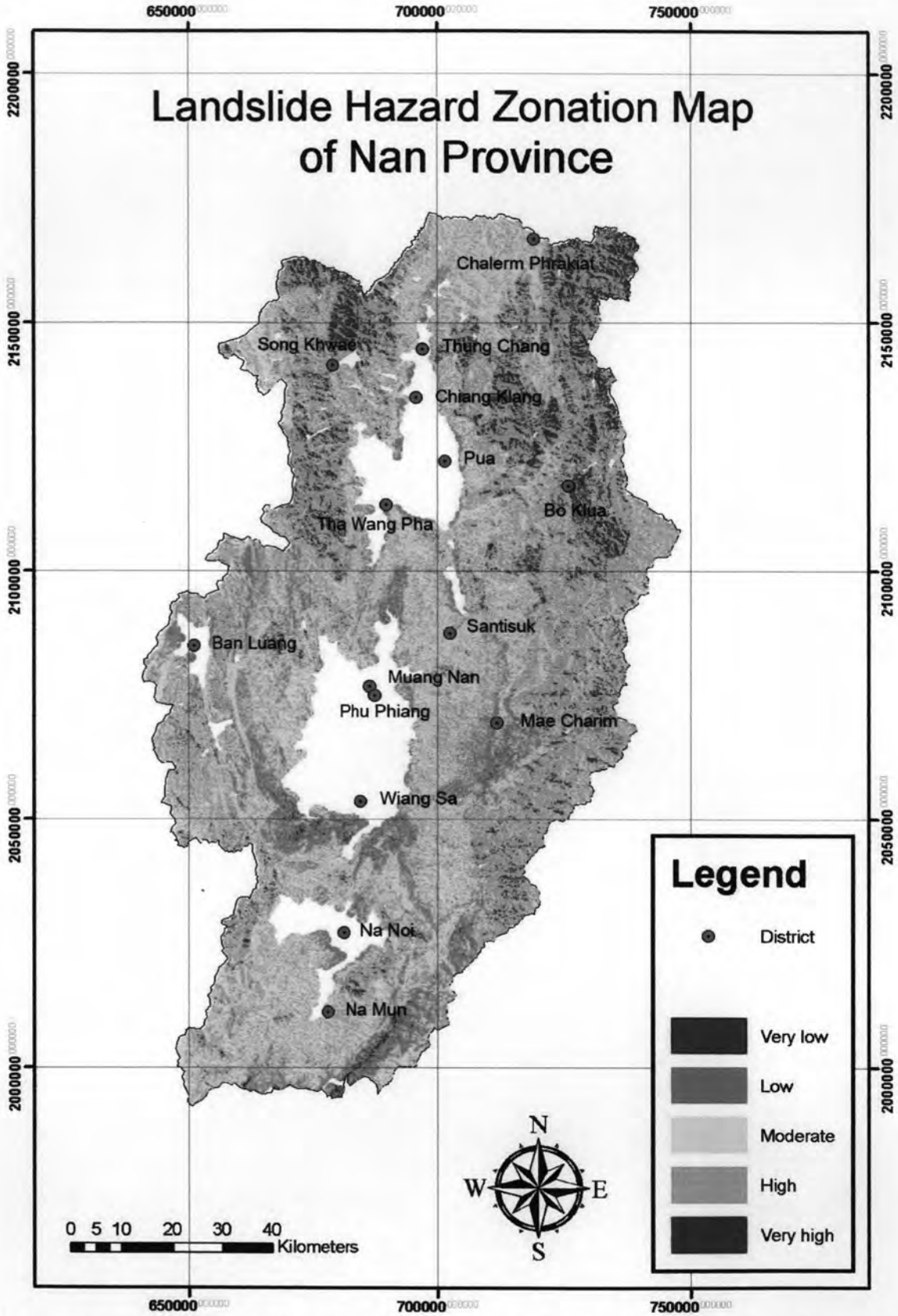

Figure 4.23 Landslide hazard zonation map of the Nan study area based on reliability probability weighting method.

4.4 Verification of the Result

The verification method is performed by comparison of existing landslide data with landslide hazard map by cross tabulation using probability method in GIS environment. The validation results show satisfactory agreement between the landslide hazard map based on reliability weighting and existing landslide location data.

The verification of probability analysis result is shown in Table 4.5. At a Landslide Probability Index (LPI) value below 0.83, the occurrence probability ratio (Ls/a) is very low and low with values of 0.23 to 0.36. The LPI index value above 1.07, the occurrence ratio is high and very high, with values of 1.34 to 3.89. The LPI index value between 0.84 - 1.06 is equal to the occurrence ratio of 1. It represents the mean landslide incidence value for the whole area. In this case, the probability indexes of dependent hazard level output are conformed to the method of probability analysis, so the method can be applied well to the landslide occurrence analysis.

Table 4.5 Comparison of landslide occurrence and landslide hazard map of the Nan study area based on reliability weighting and probability method.

Class	Hazard level	LPI	Landslide (point)	% Point of Landslide (Ls)	% of Area (a)	Ls/a =Pr
0	No Hazard	0.00	0	0.00	16.16	0.00
1	Very Low	0.36 – 0.59	1	0.05	0.24	0.23
2	Low	0.60 – 0.83	63	3.48	9.47	0.36
3	Moderate	0.84 – 1.06	642	35.45	35.71	1.00
4	High	1.07 – 1.29	846	46.71	34.75	1.34
5	Very High	1.30 – 1.53	259	14.31	3.67	3.89
Total			**1,811**	**100**	**100**	

LPI = Landslide Probability Index